frontiers in Environmental Science

ORIGINAL RESEARCH
published: 26 October 2021
doi: 10.3389/fenvs.2021.728489

Spatiotemporal Variability of the Nitrous Oxide Concentrations and Fluxes From a Cascaded Dammed River

Shengnan Wu[1,2,3†], *Xiaofeng Wang*[1,2,3*†], *Tingting Liu*[1,4], *Yixin He*[5,6], *Ziyi Que*[1,2,3], *Jilong Wang*[1,2,3], *Hang Li*[1,2,3], *Lele Yu*[1,2,3], *Yuanyuan Zhang*[1,2,3] *and Xingzhong Yuan*[1,2,7*]

[1]*Chongqing Key Laboratory of Wetland Science Research of the Upper Reaches of the Yangtze River, Chongqing, China,* [2]*Three Gorges Reservoir Area Earth Surface Ecological Processes of Chongqing Observation and Research Station, Chongqing, China,* [3]*School of Geography and Tourism, Chongqing Normal University, Chongqing, China,* [4]*State Key Laboratory of Estuarine and Coastal Research, East China Normal University, Shanghai, China,* [5]*Key Laboratory of Mountain Ecological Restoration and Bioresource Utilization and Ecological Restoration Biodiversity Conservation, Key Laboratory of Sichuan Province, Chengdu Institute of Biology, Chinese Academy of Sciences, Chengdu, China,* [6]*Zoige Peatland and Global Change Research Station, Chinese Academy of Sciences, Hongyuan, China,* [7]*Faculty of Architecture and Urban Planning, Chongqing University, Chongqing, China*

OPEN ACCESS

Edited by:
Lee E. Brown,
University of Leeds, United Kingdom

Reviewed by:
Patrick Höhener,
Aix Marseille Université, France
Wenzhi Liu,
Wuhan Botanical Garden (CAS), China

***Correspondence:**
Xiaofeng Wang
xiaofeng6540@gmail.com
Xingzhong Yuan
xzyuancqu@163.com

†These authors have contributed equally to this work and share first authorship

Specialty section:
This article was submitted to Biogeochemical Dynamics, a section of the journal Frontiers in Environmental Science

Received: *21 June 2021*
Accepted: *20 September 2021*
Published: *26 October 2021*

Citation:
Wu S, Wang X, Liu T, He Y, Que Z, Wang J, Li H, Yu L, Zhang Y and Yuan X (2021) Spatiotemporal Variability of the Nitrous Oxide Concentrations and Fluxes From a Cascaded Dammed River. Front. Environ. Sci. 9:728489. doi: 10.3389/fenvs.2021.728489

Rivers have been largely considered as the source of nitrous oxide (N_2O) to the atmosphere. N_2O emissions from rivers could be seriously influenced by damming and exhibit unique spatiotemporal patterns in river-reservoir systems. Multiple research studies report N_2O emissions from rivers with single reservoirs, but the spatiotemporal patterns and controls of N_2O emissions from cascaded river-reservoir system remain unclear. In this study, we investigated the spatiotemporal variations of N_2O concentrations and fluxes along a cascade damming river (Wubu River) in Southwest China. Our results showed that N_2O concentrations in the Wubu River ranged from 2.5 to 283.2 nmol L^{-1} with a mean of 50.7 ± 52.3 nmol L^{-1} and were generally supersaturated with gas fluxes ranging from 11.8 to 805.6 μmol m^{-2} d^{-1}. N_2O concentrations and fluxes showed a significant longitudinal variation with increasing fluxes from upstream to downstream. Meanwhile, for each river-reservoir-released water continuum, local variation of N_2O concentrations was also prominent. Reservoir sections and released water sections had 2.7 (1.2–7.9) and 3.4 (1.3–12.2) times higher N_2O concentrations than the corresponding upstream river reaches and acted as hotpots for N_2O emission. The N_2O concentrations had significant correlations with organic carbon, phosphorus, and *Chl-a* in surface water. Furthermore, the N_2O concentrations and fluxes in reservoirs had a significant correlation with hydraulic residence time and hydraulic load, suggesting that fragmentation of hydrologic conditions was an important driver for the spatial variations of N_2O concentrations in the Wubu River cascade reservoirs. Our results suggested that hydraulic residence time could predict the variation pattern of N_2O fluxes in this small river basin. Seasonal variations of N_2O concentrations and fluxes were the highest in autumn and lowest in winter and were mainly attributed to temperature and rainfall. N_2O fluxes were much higher in the Wubu River than the average levels of China's reservoirs and global reservoirs, acting as enhanced N_2O emitter. Our study highlighted that the

cascade reservoirs not only act as exciters for N_2O production and emissions but also form cumulative effects and local hotpots along the longitudinal dimension, which could significantly increase the complexity of the spatiotemporal variability in riverine N_2O emissions. Given the increasing construction of new river dams due to growing energy demand, more research should be done to quantify the contribution of cascaded damming to riverine N_2O budgets.

Keywords: cascaded damming, dissolved N_2O concentration, emission, river-reservoir-released water system, spatiotemporal variation, hydraulic residence time

INTRODUCTION

Nitrous oxide (N_2O) is an important greenhouse gas with a global warming potential nearly 300 times that of carbon dioxide, seriously accounting for the depletion of stratospheric ozone and global warming (Ravishankara et al., 2009; Alexander et al., 2013). The current atmosphere N_2O concentration (with a mean of 331 ppb) is nearly 23 and 10% higher than the preindustrial level and the level in 2000 (World Meteorological Organization, 2019). N_2O concentration in the atmosphere is still rising at a rate of 0.73 ± 0.03 ppb yr^{-1} until now (Bala et al., 2013; Ye et al., 2016). The global river ecosystem functions as important sinks and bioreactors of terrestrial nitrogen, making them important emitters of N_2O to the atmosphere *via* powerfully nitrogen processing (Seitzinger et al., 2000; Boyer et al., 2006; Yan et al., 2010) and receiving widespread attention (Beaulieu et al., 2010; Beaulieu et al., 2011; Yu et al., 2013). Previous estimates indicated that more than 0.68 Tg yr^{-1} of nitrogen loading would be converted to N_2O by microbial metabolism in the global rivers, which is equivalent to 10% of the global anthropogenic N_2O emissions (Beaulieu et al., 2011; Rosamond et al., 2012). Furthermore, increasing human activities have been gravely altering the global balance of nitrogen through fertilizer production and application, particularly leading to more and more nitrogen-rich runoff into inland water and subsequent enhancement of N_2O emissions. It is predicted that continuously growing nitrate concentration in global rivers will cause riverine N_2O emissions to further increase by about 40% (Trauth et al., 2018). More importantly, humans have affected riverine nitrogen biogeochemical processes not only by enhancing nonpoint or point nitrogen loading to rivers but also through river damming and nitrogen retaining (Van Cappellen and Maavara, 2016). Riverine N_2O emissions are strongly influenced by river damming and hydrology (Guérin et al., 2008; Beaulieu et al., 2010; Zhu et al., 2013), exhibiting intense variability and complexity. Hence, the estimation of N_2O emissions from rivers worldwide and their contribution to the global N_2O budget still suffers from high uncertainties given the complex human interference (Beaulieu et al., 2010; Wang et al., 2017b; Shi et al., 2020).

Damming of river, one of the most important factors affecting river ecosystems, has a significant impact on the hydrology, water environment, nutrients transportation and distribution, and hydraulic residence time. Thus, it imposes a strong influence on nitrogen distribution, denitrification, and related N_2O emissions (Beaulieu et al., 2014; Cheng et al., 2019; Middelburg, 2020). In the past decades, the number of dams has been booming for a series of purposes, including hydropower generation, water resource management, flood control, irrigation, and navigation. There are at least 70,000 large dams and countless small reservoirs having been built worldwide, significantly altering the physical structure and nutrient cycling of river ecosystems (Maavara et al., 2015). River segmentation and disruption by dams, accompanied by decreasing flow velocity, increasing hydraulic retention time, and trapping terrestrial nutrients, could cause the accumulation of sediments and nutrients in reservoirs and thereby alter the nitrogen biogeochemical cycle (Maeck et al., 2013). Owing to the increasing damming on global rivers, the total amount of carbon, nitrogen, and phosphorus transported from land to ocean would decrease by 19, 14, and 17% until 2030, respectively (Maavara et al., 2015; Maavara et al., 2017; Akbarzadeh et al., 2019). More recently, Beusen et al. (2016) estimated that approximately 1929 Gmol N yr^{-1} could be detained and eliminated in river systems *via* burial and denitrification, while 24% of which (463 Gmol N yr^{-1}) take place in reservoirs. Akbarzadeh et al. (2019) estimated the total nitrogen retained in reservoirs worldwide of around 270 Gmol N yr^{-1} in 2000; the value will increase by 467 Gmol N yr^{-1} by 2030 as a result of the completion of dams that are currently under construction or being planned. Such a quantity of nitrogen trapped in reservoirs can stimulate *in situ* denitrification and nitrification-denitrification (Beaulieu et al., 2015; Akbarzadeh et al., 2019; Liang et al., 2019); combining with the increased hydraulic residence time and water depth and accompanying dissolved oxygen stratification, damming observably turns rivers into hotspots of N_2O emissions (Liu et al., 2011a; Liang et al., 2019). Furthermore, river damming can modify carbon richness and bioavailability and thereby carbon-nitrogen ratio, exerting a strong influence on microbial denitrification and nitrification and concomitant N_2O production (Shi et al., 2020). A study by Shi et al. (2020) showed that the abundance of denitrifying bacteria in reservoir sediments with prolonged residence time was much higher than those upper nature rivers; as a result, significantly high N_2O fluxes from reservoir reaches. Cheng et al. (2019) also found that dams construction caused the reservoir reaches to be hotspots for N_2O emissions along the Yellow River due to more retention and decomposition of particle nitrogen and organic nitrogen. Except for the above, river damming often forms a specific pathway for

N_2O emissions *via* the water released from reservoir hypolimnion (Liu et al., 2009b). Overall, damming river has been considered to create a specific spatiotemporal pattern of riverine N_2O generations and emissions. However, studies on N_2O emissions from river-reservoir system are insufficient in view of various river types and a tremendous number of dams all over the world.

As a matter of fact, many existing dams have been built as a cascade configuration for more adequate water energy development (He et al., 2019). Cascade hydropower development is the key strategy in many developing countries, especially in China, for energy supply, climate-change mitigation, and economic development. However, multiple research studies have focused on N_2O emissions from rivers with single reservoirs, but the cascaded river-reservoir systems remain less attention (Liu et al., 2011a; Zhu et al., 2013; Cheng et al., 2019; Liang et al., 2019; Shi et al., 2020). Cascade damming, leading to a series of successive "river-reservoir-release" systems along river mainstream, can generate refilter and redistribute for the transportation of C, N, and P along the river continuum (Chen et al., 2020). The dynamic processes and spatial patterns of N_2O emissions in cascade river-reservoirs systems are thus more complex than single reservoir-river system (Jin et al., 2018; Liang et al., 2019; Shi et al., 2020; Wu et al., 2020; Yang et al., 2020). Particularly, Liang et al. (2019) found that cascade damming and accompanying fragmentation of hydraulic load significantly dominated exceptionally spatial variability of N_2O fluxes in the cascade reservoirs along the Wujiang River in Southwest China, implying significant differences between reservoirs and rivers. Shi et al. (2020) also found that the downstream reservoirs showed higher N_2O fluxes due to the continuous accumulation of inorganic nitrogen derived from organic nitrogen mineralization along the cascade reservoirs in the upper Mekong River. Meanwhile, Jin et al. (2018) proposed that the significantly longitudinal discontinuities in riverine N_2O emissions due to cascade damming could affect the estimation of the total emissions. Obviously, cascade dams may lead to dual spatial variation patterns of N_2O emissions in river-reservoir systems. Yet despite all that, previous studies have focused on cascade damming in the large rivers (e.g., Wujiang River, Mekong River, and Han River) (Jin et al., 2018; Liang et al., 2019; Shi et al., 2020; Wu et al., 2020), while in these studies, the N_2O emissions are strongly disturbed by watershed environment changes due to overlong flow lines. Thus, the spatiotemporal patterns and controls of N_2O emissions from cascade river-reservoir systems remain unclear, and relevant studies in small river catchments are quite essential.

As one of the most flexible and sustainable energy sources, hydropower has been actively pursued worldwide in recent years, and the cascade hydropower has already become an effective means to meet increasing energy demands. In the late 20th century, the Chinese government has encouraged and proposed a great deal of cascade hydropower plans and constructions for rural power supply and irrigation (Chang et al., 2010; Grumbine and Xu, 2011). There are many relatively stable "river-reservoir-river-reservoir" systems providing good conditions for exploring the long-term ecological impact of cascade hydropower development. We hypothesized that N_2O emissions may differ in cascade reservoirs and in river sections vs. reservoir sections as a result of the alterations in water residence time by cascade damming and related N geochemical and biological factors. In this study, we investigated the spatiotemporal variations of N_2O concentrations and fluxes from a typical cascade damming river with small river catchment in Southwest China. The objectives of this study were to 1) identify the spatiotemporal variability of N_2O emissions in cascaded small reservoirs and 2) explore the main controls for the N_2O patterns. Our results also provide scientific reference on N_2O emissions characteristics and total amount estimation from the global freshwater ecosystem.

MATERIALS AND METHODS

Study Area

The study was conducted in a small mountain river, Wubu River (28°10′-32°13′N, 105°11′-110°11′E), which is a southern tributary of the Yangtze River located in Chongqing, Southwest China. It has a length of 82 km, a watershed area of 856 km^2, and an average slope of 5.3‰ with the total fall between river ends amounting to 800 m (Wang et al., 2019). The area features a subtropical monsoon humid climate with multiyear average temperature of 18.3°C and annual precipitation of 1,133 mm (Ren et al., 2016). Three main tributaries are distributed in the Wubu River, which are named Ersheng stream, Ya stream, and Lugou stream, respectively. The annual average discharge in the Wubu River estuary is monitored at about 13.8 m3 s^{-1} (Ren et al., 2016). Forest and farmland are the main types of land use; few sporadic urban lands are distributed in the downstream area. Despite small watershed, the Wubu River mainstream and its tributaries have been heavily dammed for hydropower production and irrigation in the past 50 years. Up to 2014, over 15 small dams were constructed in the whole catchment and at least three cascaded dams in each tributary.

Sites Description

Based on the current status of all dams in the Wubu River basin, five cascaded reservoirs along the Wubu River mainstream, including Chaeryan (R1), Xiaoguan (R2), Jianghe (R3), Xitan (R4), and Yangjiadong (R5), were investigated. Meanwhile, three reservoirs downstream of the Ersheng stream (R6), Ya stream (R7), and Lugou stream (R8), respectively, were also selected (**Figure 1**). There are a total of eight "river-reservoir-released water" systems shown in **Figure 1**. R1 and R2 represented upstream reservoirs, while R4–R8 were defined as downstream ones. The main features of these cascade reservoirs are presented in **Table 1**. All dams were constructed for power generation during 1950–1980. The selected dams are relatively small in size, with heights and lengths ranging from 4 to 19 m and from 22 to 90 m, respectively (**Table 1**; **Supplementary Table S1**). The hydraulic residence time in reservoirs (only 0.49–3.77 days) is much shorter compared to other large reservoirs (Liang et al., 2019). Furthermore, there is inconspicuous stratification in R1–R5 and R8 because of relatively shallow water depth and

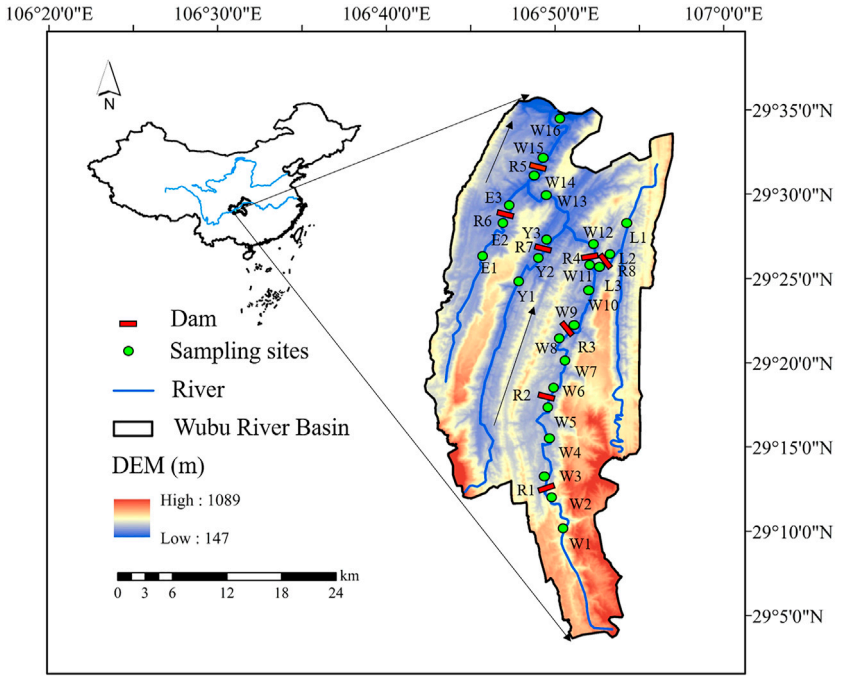

FIGURE 1 | Sampling locations and sites in the Wubu River basin. The short red lines denote dams and green dots signify sampling sites.

TABLE 1 | The main features of cascade hydropower reservoirs in the Wubu River basin.

	R1	R2	R3	R4	R5	R6	R7	R8
Construction time	1979	1969	1984	1980	1977	1959	1980	1975
Dam height (m)	8	8	6	7.5	12	12	19	16
Effective dam lengths (m)	22	40	38	57	90	58	55	37
Backwater distance (km)	0.6	0.6	1.4	1.2	2.53	3.2	1.1	0.8
Dewater length (km)	0.6	—	—	0.15	0.0	0.2	—	—
Installed capacity (MW)	0.45	4.0	0.32	0.52	0.60	0.20	0.07	0.36
Mean water depth (m)	3.2	2.5	3.3	4.2	3.4	5.6	6.4	3.4
Total capacity (×105 m^3)	2	3.7	8.3	13.5	28.0	7.6	2.3	1.6
Discharge (×105 m^3 d^{-1})	4.1	4.3	5.8	6.8	9.9	1.5	1.6	1.0
Hydraulic residence time (*HRT*, d)[a]	0.49	0.85	1.42	1.64	1.58	5.11	1.46	1.61
Hydraulic load (*H*, m d^{-1})[b]	6.58	2.90	2.30	2.59	2.17	1.09	4.39	2.13

[a]*Hydraulic residence time was derived by dividing total storage capacity by the averaged interflow discharge of each reservoir.*

[b]*Hydraulic load is the ratio of the mean water depth to the residence time. All data were derived from the "Hydropower resources development plan of small and medium rivers in Chongqing."*

short hydraulic residence time. R6 has the longest residence time and smallest hydraulic load. All the eight reservoirs have experienced various degrees of eutrophication in autumn and spring (**Supplementary Table S2**). We segmented each river-reservoir system into three different sections, standing for the inflowing river (the intermediate riverine reaches between the dams), the reservoir (in front of the dam), and released water (within 300 m downstream of each dam), respectively, to perform the seasonal investigations on chemical parameters and N_2O concentrations in surface water. Meanwhile, an extra section was selected in the estuary of the Wubu River. Thus, there were a total of 25 sections including 16 sections in mainstream named W1–W16 along the flow direction and nine sections in Ersheng stream (E1–E3), Yaxi stream (Y1–Y3), and Lugou stream (L1–L3) (**Figure 1**). In each selected section, we deployed three sampling sites at the central and both flanks of the river, resulting in a total of 75 sampling sites. Detailed hydrological parameters in each sampling section were shown in **Supplementary Table S1**.

Sample Collection

The four sampling campaigns were carried out in September 2014 (autumn), December 2014 (winter), March 2015 (spring), and June 2015 (summer) at 75 sites. During each sampling campaign, a surface water sample (500 ml, upper 0.3 m) was collected using an organic glass hydrophore and stored in acid-washed

polyethylene bottles for water chemistry parameters analyses. Then, a graduated syringe was employed to collect and inject another 100 ml of surface water into 200 ml aluminum foil gas bag for dissolved N_2O analysis. Immediately, we injected 0.2 ml of saturated $HgCl_2$ into the aluminum foil gas bag to inhibit microbial metabolism. Triplicate water samples were collected at each sampling site. All water samples were stored in the incubator at 4°C and analyzed within 5 days.

During field surveying, triplicate 180 ml *in situ* atmospheric samples at 1 m above the river surface were collected and injected into gas sample bags for atmospheric background concentration measurement. Meanwhile, *in situ* water temperature (WT), dissolved oxygen (DO), conductivity (Con), and chlorophyll-a (*Chl-a*) were measured by the calibrated Manta™2 Multiparameter System (Eureka Company, United States). Moreover, wind speed (u) and air temperature (AT) at 1 m above the water surface were measured by the anemogram (Kestrel 2,500, United States).

Sample Analysis

In this study, total nitrogen (TN), ammonium-nitrogen (NH_4^+-N), nitrate-nitrogen (NO_3^--N), total phosphorus (TP), dissolved total phosphorus (DTP), and orthophosphate (PO_4^{3-}) in water were determined according to the Monitoring Analysis Method of Water and China's State Environmental Protection Wastewater (China's State Environmental Protection, 2002). The measurements of total organic carbon (TOC) and dissolved organic carbon (DOC) in water were performed by the TOC analyzer (Multi N/C 2100, Jena, Germany). For the measurements of NH_4^+-N, NO_3^--N, dissolved inorganic nitrogen (DIN), DTP, PO_4^{3-}, and DOC, water samples were filtered through 0.45 μm cellulose acetate membranes. Triplicate determinations of all samples were performed to estimate the analytical precision. The assured precision was better than 5%. The precision of the TOC analyzer was about 0.001 mg L^{-1}.

The modified headspace equilibrium method was employed to determine the dissolved N_2O concentrations in this study (Clough et al., 2007; Wang et al., 2009b). Firstly, 80 ml of ultrapure N_2 was injected into the aluminum foil gas bag that was filled with 100 ml water sample to create a headspace. The gas bag was then shaken violently for 5 min to let dissolved N_2O diffuse out and equilibrated for 10 min for equilibrium between the headspace and water phases (Koschorreck et al., 2021). Whereafter, we extracted 20 ml of headspace gas for analyzing the N_2O concentration by gas chromatograph (Agilent 7890A, Agilent Co., United States). The gas chromatograph is equipped with an electron capture detector (ECD detector) and a 1 1 m × 2 mm packed Porapak Q (80/100 mesh) column. The column and the ECD detector were operated at 50 and 350°C, respectively. The concrete operations of gas chromatograph were described in a previous study (Zhu et al., 2015). The system was certified with commercial gas standards in 4.9 ppb after measuring every six consecutive samples. The minimum detectable N_2O concentration was 1×10^{-3} ppb.

N_2O Concentration and Flux Calculations

Calculations of N_2O Concentration and Saturation

The dissolved N_2O concentrations in water (c_w) were calculated using the equation described by (Yu et al., 2013; Wang et al., 2017b):

$$c_w = (c_a \times V_a + a \times c_a \times V_w) \div V_w \quad (1)$$

where C_a is the N_2O concentration in the headspace during equilibration (nmol L^{-1}), V_a is the volume of headspace (0.08 L), V_w is the volume of water sample in the gas sample bag (0.10 L), and a is the Bunsen coefficient of N_2O adjusted for temperature (Weiss and Price, 1980). Then, we calculated the N_2O saturation (s) *via* dividing dissolved N_2O concentrations in the water sample (c_w, in nmol L^{-1}) by the N_2O concentrations in the surface water that is in equilibrium with the atmospheric concentration (c_s, in nmol L^{-1}). Here, c_s is calculated according to Henry's law using temperature-dependent solubility (Weiss and Price, 1980). The equations were as follows:

$$s = c_w \div c_s \times 100\% \quad (2)$$

$$c_s = a \times c_a \quad (3)$$

Calculation of N_2O Flux

In this study, the fluxes of N_2O at the water-air interfaces were calculated *via* the classic boundary-layer model (Liss and Slater, 1974), which has been widely used in other studies on riverine N_2O emissions (Cole and Caraco, 2001; Wang et al., 2009b; Wang et al., 2017b). Here, we hypothesized gas exchange only through molecular diffusion obeying Henry's law. The calculations of N_2O flux were performed according to the following equation:

$$F = k_0 (c_w - c_s) \quad (4)$$

where F is N_2O flux (μmol m^{-2} d^{-1}), c_w is the measured N_2O concentration in water (nmol L^{-1}), c_s is the theoretical dissolved concentration of N_2O in water (nmol L^{-1}) when water-air equilibrium is reached, and k_0 is the gas transfer velocity (m d^{-1}) at the air-water interface. The gas transfer velocity was calculated according to the following function (Wanninkhof, 1992):

$$k_0 = k_{600} \times (S_C \div 600)^{-n} \quad (5)$$

$$S_C = 2301.1 - 151.1 \times t + 4.7364 \times t^2 - 00.059431 \times t^3 \quad (6)$$

where *Sc* is the Schmidt number for N_2O adjusted by *in situ* WT; $n = 0.66$ or 0.5 for wind speeds ≤3 or >3 m s^{-1}; t is the *in situ* WT (in °C); and k_{600} is the piston velocity normalized for N_2O with a Schmidt number of 600.

Previous studies suggested that k_0 was mainly controlled by the basin physical feature (including water depth, flow velocity, and slope) and wind speeds (Raymond and Cole, 2001; Borges et al., 2004; Clough et al., 2007), which are all correlated with water turbulence. As thus, scholars have attempted to construct some empirical models for k_0 calculation based on wind speed or hydrological factors for more precise estimations of the N_2O emissions from river water to atmosphere (Raymond and Cole, 2001; Borges et al., 2004). While the functions of wind speed for k_0 calculation were widely used in the water with low flow velocities and large areas, hydrological functions were mostly applied in rivers and streams with small water surface and high flow velocity (Raymond and Cole, 2001; Clough et al., 2007). Since flow velocity and water depth were obviously different among the river, reservoir, and released water section, it was likely

TABLE 2 | Detailed spatial variations in environmental parameters in the Wubu River basin.

Water quality parameters	Mainstream																Tributary								
	R1			R2			R3			R4			R5			Est	R6			R7			R8		
	w1	w2	w3	w4	w5	w6	w7	w8	w9	w10	w11	w12	w13	w14	w15	w16	E1	E2	E3	Y1	Y2	Y3	L1	L2	L3
WT/°C	19.26	19.63	19.87	20.55	20.33	20.71	21.20	20.95	21.17	22.82	22.32	22.73	22.49	22.16	22.98	22.76	22.23	21.72	22.98	19.27	19.70	20.19	21.39	20.90	21.94
pH	7.89	7.97	7.83	7.83	7.93	7.75	7.91	8.06	7.90	8.03	8.22	8.00	8.01	8.19	8.01	8.14	7.80	8.15	7.95	8.18	8.41	8.21	8.35	8.41	8.25
Con/ μS cm^{-1}	314.1	335.4	326.1	341.4	350.3	339.3	330.6	365.2	358.8	410.6	684.5	547.3	550.9	557.8	543.4	465.0	322.0	324.5	319.1	382.8	435.6	418.2	394.9	434.1	426.5
DO/mg L^{-1}	7.26	7.94	7.21	6.61	7.48	7.05	7.42	8.39	7.47	7.55	9.56	7.92	7.67	8.41	7.33	7.71	7.37	8.68	7.76	8.22	8.87	8.18	7.78	8.16	7.83
Chl-a/μg L^{-1}	1.65	3.71	1.77	1.80	4.29	1.84	1.80	5.33	2.37	1.56	7.31	2.47	2.33	11.13	6.49	8.42	4.07	27.26	11.68	3.11	6.57	3.58	1.94	3.20	2.48
TN/mg L^{-1}	2.25	2.75	3.00	2.95	3.37	3.38	2.91	3.21	3.09	3.12	3.19	3.27	3.91	3.93	3.96	3.57	2.96	2.68	2.92	4.48	3.11	2.91	1.68	3.54	3.29
NO_3^-/ mg L^{-1}	1.24	1.58	1.64	1.52	2.10	1.86	1.95	1.62	1.70	1.38	1.97	1.74	2.17	1.59	1.65	2.36	2.16	1.36	2.11	2.67	2.17	2.45	1.27	2.19	2.16
NH_4^+/ mg L^{-1}	0.05	0.09	0.08	0.07	0.10	0.10	0.11	0.13	0.13	0.16	0.15	0.19	0.20	0.18	0.16	0.24	0.24	0.24	0.24	0.34	0.34	0.40	0.05	0.09	0.10
TP/mg L^{-1}	0.06	0.07	0.07	0.07	0.08	0.07	0.07	0.08	0.08	0.08	0.10	0.09	0.10	0.10	0.10	0.12	0.13	0.17	0.16	0.13	0.19	0.20	0.06	0.12	0.10
DTP/mg L^{-1}	0.04	0.05	0.06	0.06	0.08	0.07	0.05	0.06	0.07	0.06	0.08	0.08	0.09	0.10	0.10	0.09	0.06	0.09	0.08	0.08	0.11	0.10	0.04	0.08	0.08
PO_4^{3-}/ mg L^{-1}	0.02	0.03	0.03	0.04	0.04	0.04	0.03	0.04	0.04	0.03	0.04	0.04	0.05	0.06	0.06	0.05	0.03	0.06	0.05	0.04	0.06	0.05	0.03	0.05	0.05
DOC/mg L^{-1}	6.92	8.10	7.11	9.55	12.55	11.86	11.52	17.54	14.88	15.67	18.88	17.06	13.96	20.01	17.25	19.15	8.88	17.66	16.20	7.64	13.35	11.78	7.35	18.30	15.91
TIC/mg L^{-1}	40.55	36.00	36.30	39.10	28.55	27.83	32.69	19.68	22.33	32.48	27.28	26.58	40.78	25.70	32.08	34.93	29.04	15.38	17.93	51.45	18.53	24.35	43.84	30.15	29.68
TOC/mg L^{-1}	10.15	14.96	12.63	19.61	24.17	16.03	16.53	24.04	18.47	24.83	23.41	20.78	19.51	25.67	25.57	31.71	12.71	25.41	21.75	16.51	19.28	18.35	16.97	23.66	21.78
C/N	4.52	5.43	4.21	6.64	7.18	4.74	5.68	7.49	5.97	7.97	7.34	6.36	4.99	6.54	6.46	8.89	4.29	9.47	7.44	3.68	6.20	6.30	10.09	6.69	6.61
N/P	38.22	41.68	46.09	43.12	40.93	51.46	39.82	39.63	40.17	38.53	33.19	38.04	40.28	38.33	40.04	30.88	23.20	16.07	17.80	34.50	16.25	14.25	27.28	29.50	31.90

that simple models based on wind speed or hydrological factors were inapplicable in our study. Particularly, the flow velocity and turbulence were strongly enhanced downstream of dams (**Supplementary Table S1**). And thus, the k_0 values in our study were calculated using an integrated empirical model that was based on both wind speed and hydrological factors (Clough et al., 2007):

$$ko = 17.19 \times (v \div h)^{0.5} + 0.31 \times U_{10} \times (S_C \div 600)^{-0.5} \quad (7)$$

where v is the measured flow velocity (m s^{-1}), h is water depth (m), and U_{10} is the wind speed at a height of 10 m above the water surface (ms^{-1}). The hourly measurements of wind speed were gained from the weather station in the watershed. The flow velocity varied with the seasonal precipitation and the dam position (**Supplementary Table S1**).

Statistical Analysis

Excel 2010 was employed in this study to calculate the initial data. SPSS 23.0 (SPSS Inc.) was used for all of the statistical analyses. The data were tested for normality distribution with the Kolmogorov–Smirnov test. If abnormal distribution, the data should be *ln*-transformed before statistical analysis. The statistically significant differences in N_2O concentrations and fluxes among seasons, sampling sites, or each river-reservoir-released water system were tested using the one-way analysis of variance (ANOVA) and paired-samples T-tests (pairwise comparison). Pearson correlation analysis and stepwise multiple regression were used to determine the relationships between environment factors and hydraulic conditions with N_2O concentrations and fluxes. Meanwhile, all artworks were plotted by GraphPad Prism 8.

RESULTS

Water Quality Parameters

The characteristics of the measured water chemistry variables are listed in **Table 2** and **Supplementary Figures S1–S3**. TN, NO_3^-, and NH_4^+ in all water samples ranged from 1.32 to 6.78 mg L^{-1}, 0.87 to 3.50 mg L^{-1}, and 0.02 to 0.69 mg L^{-1}, respectively, and presented increasing trends along the flow direction in the mainstream of the Wubu River (**Supplementary Figure S3**). In each river-reservoir-released water system, N concentrations in reservoir sections and released water sections were higher than those in inflowing river sections, with the exception of the R6 and R7. Particularly, the proportion of NO_3^- and NH_4^+ in TN showed clear trends of increasing from the upstream reservoir to downstream ones, indicating the accumulated characteristic of dissolved inorganic nitrogen downstream. Meanwhile, the TP, DTP, and PO_4^{3-} fell in the scope of 0.04–0.16 mg L^{-1}, 0.02–0.14 mg L^{-1}, and 0.01–0.08 mg L^{-1}, respectively, showed a relatively low level (≤0.20 mg L^{-1}), and still presented a weak increase along longitudinal dimension, while in most of the reservoir systems, there was no significant difference among the river, reservoir, and released water sections. TOC and DOC concentrations in reservoir sections were generally higher than those in their inflowing river sections.

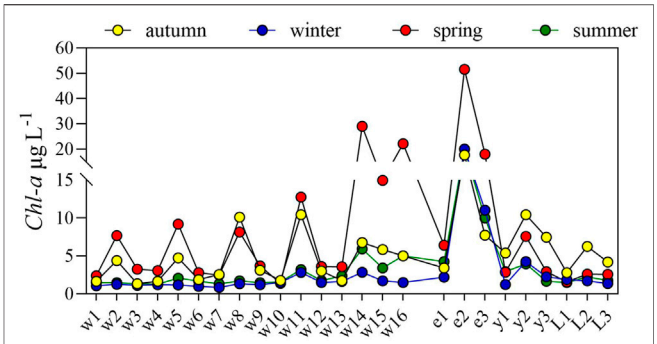

FIGURE 2 | Spatial and temporal distribution of *Chl-a* in the river-reservoir system along the Wubu River and its tributaries.

In addition, *Chl-a* concentration in downstream reservoirs (e.g., R4, R5, R6, and R7) were extremely higher than other reservoirs and river sections, showing the current state of eutrophication, especially in warm seasons (**Figure 2**). Averaged DO in each section was in the range of 6.61–9.56 mg L^{-1} and showed a relatively high oxygen level. DO in reservoirs were slightly higher than those in the inflowing rivers. pH, DO, and conductivity all showed differentiation among cascaded reservoirs and within each river-reservoir-released water system (**Supplementary Figure S2**; **Supplementary Table S1**).

Spatial Variations of N_2O Concentrations

The dissolved N_2O concentrations in surface water presented substantially spatial variations through the whole cascaded river-reservoir systems with a wide range of 2.5–283.2 nmol L^{-1} (corresponding saturation of 38.2–3,715.1%) (**Figure 3A**). The overall averaged N_2O concentration in the Wubu River basin was 50.7 ± 52.3 nmol L^{-1} (saturation of 830 ± 797%). It was indicated that most of the sampling sites were powerfully supersaturated with N_2O and acted as net sources for atmospheric N_2O.

Dissolved N_2O concentrations in the Wubu River mainstream showed obviously longitudinal spatial variations during four investigations (**Figure 3**; **Supplementary Figure S4**), presenting an obviously increasing trend from upstream reservoirs to downstream ones. Variance analysis indicated that N_2O concentrations in R4 (average of 83.3 ± 62.1 nmol L^{-1}) and R5 (average of 65.0 ± 49.5 nmol L^{-1}) were significantly higher than those in R1 (20.1 ± 11.1 nmol L^{-1}), R2 (23.7 ± 13.6 nmol L^{-1}), and R3 (29.6 ± 24.0 nmol L^{-1}). Meanwhile, downstream reservoirs on three tributaries also had comparable N_2O concentrations with R4 and R5, with averaged values in R6, R7, and R8 of 87.1 ± 91.1 nmol L^{-1}, 40.4 ± 30.8 nmol L^{-1}, and 57.9 ± 51.8 nmol L^{-1}, respectively. Downstream reservoirs formed hotspots of N_2O emissions in the Wubu River basin.

For each river-reservoir-released water system, dissolved N_2O concentrations showed obvious variation among different hydrological sections. The N_2O concentrations in all river sections were averaged at 23.2 ± 17.8 nmol L^{-1} (ranging from 2.5 to 78.6 nmol L^{-1}), significantly lower than those in the

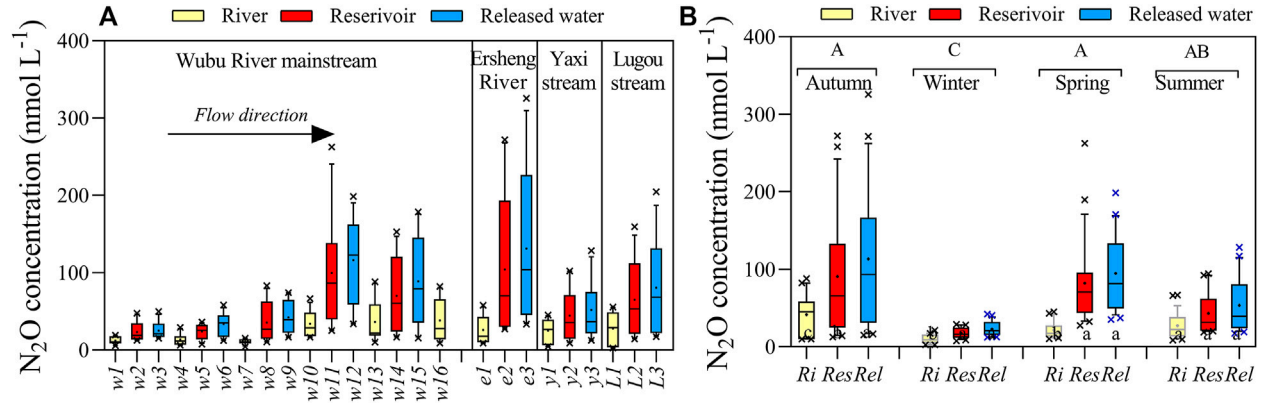

FIGURE 3 | (A) Spatial and temporal distributions of N_2O concentrations in the river-reservoir system along the Wubu River and its tributaries. The box extent, error bars, and line and plus sign inside the box denote 25th and 75th percentiles, 10th and 90th percentiles, and median and mean, respectively. The capital letters in **(B)** show a significant difference among four seasons with $p < 0.05$.

reservoirs (with a mean of 58.2 ± 56.3 nmol L^{-1}, ranging from 10.2to 252.1 nmol L^{-1}, $p < 0.01$). N_2O concentrations in each reservoir section were 1.2–7.9 times (averaged 2.7 times) higher than that in their corresponding inflowing river sections, especially in spring (averaged 4.1 times, **Figure 3A**). Released water sections showed extremely high N_2O concentrations, with an average of 71.1 ± 62.6 nmol L^{-1} (ranging from 13.2 to 283.2 nmol L^{-1}), nearly 3.4 times these in inflowing river sections. In spring, dissolved N_2O concentrations in the released water of the downstream reservoirs (R4, R5, and R6) were 7.7 times higher than that in their upstream river sections. N_2O concentrations in the cascaded "river-reservoir-released water" system showed a widespread "low-high-extremely high" local pattern. A similar local pattern of N_2O concentration was also verified downstream of the three tributaries. There was, in addition, one further point that annually averaged N_2O concentrations in each released water section decreased by 20–69% (average of 47%) compared to those in the subsequent downstream river sections (e.g., w3 vs. w4; w6 vs. w7). By the assumption that there was no tributary inflowing, the obvious N_2O loss between released water and subsequent river section (**Figure 3A**, **Supplementary Figure S4**) implied mass of N_2O evasion from such reaches along the mainstream of the Wubu River. As a result, riverine N_2O concentrations exhibited a unique spatial pattern of coupling local and watershed patterns under cascaded damming.

Seasonal Variations in the N_2O Concentrations

N_2O concentrations in the Wubu River exhibited significantly seasonal variations (**Figure 3B**). In autumn and spring, the arithmetic mean N_2O concentrations in surface water were 80.3 ± 73.5 nmol L^{-1} (corresponding saturation of 1,088% ± 980%) and 64.4 ± 51.3 nmol L^{-1} (corresponding saturation of 1,052% ± 881%), respectively, and were markedly higher than these in summer (average of 40.5 ± 27.85 nmol L^{-1}, corresponding saturation of 918.2 ± 631%). The winter (average of 16.3 ± 8.89 nmol L^{-1}, corresponding saturation of 260.3 ± 146%) showed significantly lower N_2O concentrations than the other three seasons ($p < 0.05$). In addition, consistent seasonal patterns were found either in inflowing river sections or in reservoir and released water sections and even in the upstream channel, indicating that cascaded damming had no dominant influence on the seasonal pattern of N_2O concentration in this study. The difference of N_2O concentrations among river, reservoir, and released water sections was obviously affected by the seasonal variation. In autumn and spring, there were stronger variations of N_2O concentrations, while mitigatory variations among different hydrology sections were found in winter and summer.

N_2O Fluxes

In this study, our estimated k_0 ranged from 4.4 to 17.2 cm h^{-1} (**Supplementary Table S3**). Due to the differences in flow velocity and water depth between flowing and impounding sections, k_0 values showed a remarkable difference in river, reservoir, and released water reaches (average of 11.9, 5.8, and 12.9 cm h^{-1}, resp.). Impounding sections had significantly lower k_0 values than river and released water sections as a result of weak turbulence. Using the k_0 values and dissolved N_2O concentrations, the calculated N_2O fluxes from the Wubu River ranged from −11.8–805.6 μmol m^{-2} d^{-1} (average of 104.6 ± 98.4 μmol m^{-2}·d^{-1}). There were only four negative N_2O fluxes in all sampling sites, indicating that the Wubu River acted as a generally net N_2O source for atmosphere. Similar to N_2O concentrations, N_2O fluxes presented an increasing trend from upstream reservoirs to downstream ones, with remarkably low values from R1, R2, and R3 and strong emissions in downstream R4 and R5. N_2O fluxes from the downstream reservoirs in tributaries (R6–R7) also had higher values (**Figure 4A**). Meanwhile, the averaged N_2O fluxes from released water sections were of 194.8 ± 130.4 μmol m^{-2}·d^{-1}, and much higher than those in inflowing river sections (56.2 ± 31.81 μmol m^{-2}·d^{-1}). Reservoir sections had slightly higher N_2O fluxes of 68.8 ± 35.9 μmol m^{-2}·d^{-1} than river sections

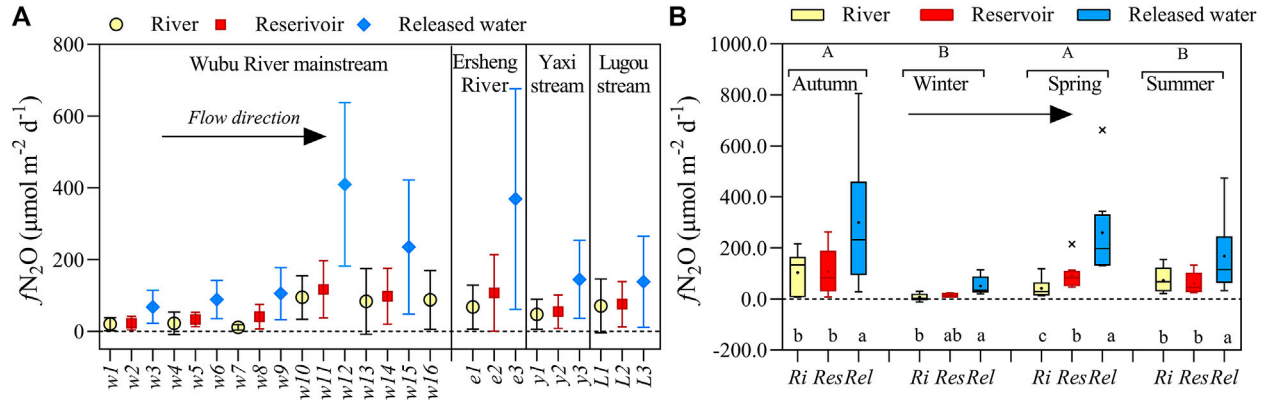

FIGURE 4 | (A) Spatial and temporal distributions of N_2O fluxes in the cascaded river-reservoir system along the Wubu River and its tributaries. The capital letters in **(B)** show the significance of difference among four seasons and lowercase letters denote the statistical significance among different hydrology sections in the same season with $p < 0.05$.

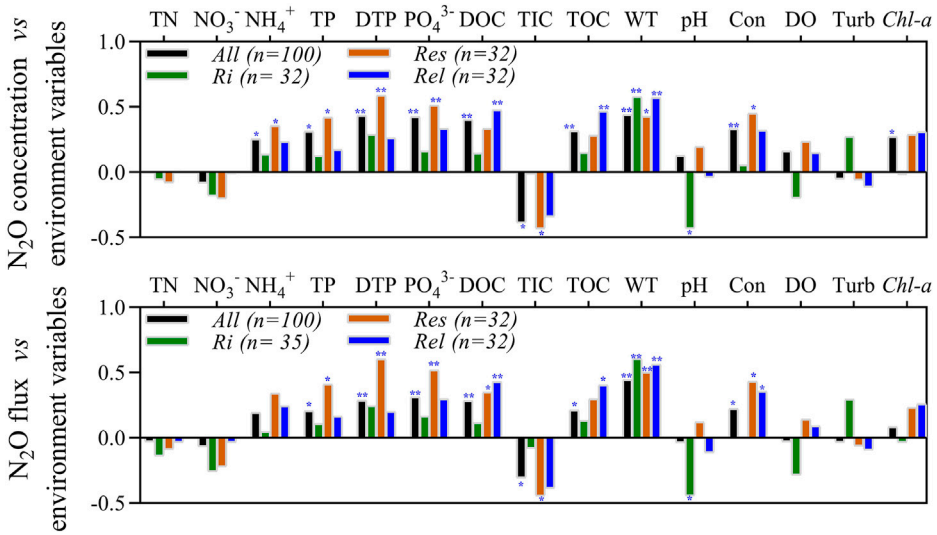

FIGURE 5 | Pearson correlation coefficient (PCC) between N_2O concentrations, fluxes, and water chemistry variables measured in the river (*Ri*), reservoir (*Res*), and released water (*Rel*) sections. "*" and "**" on the bar denote the statistical significance with $p < 0.05$ and $p < 0.01$, respectively.

when using noticeably low k_0 values. Furthermore, the highest N_2O fluxes were found in autumn (167.8 ± 178.6 μmol m^{-2}·d^{-1}) and in winter were significantly lower (23.1 ± 28.8 μmol m^{-2}·d^{-}) than those in other seasons (**Figure 4B**).

Relations With Environment Variables

The correlation analyses of dissolved N_2O concentrations with water environment factors were shown in **Figure 5**. N_2O concentrations were significantly and positively correlated with WT, conductivity (Con), *Chl-a*, NH_4^+, phosphorus (TP, DTP, and PO_4^{3-}), and carbon (TOC and DOC), while they were negatively correlated with TIC ($p < 0.05$) (**Figure 5**). There was no significant correlation between N_2O concentration with TN, NO_3^-, or DO, either in river sections or in reservoir sections, violating the expectations. When using all data points, simple linear regressions indicated that *Chl-a*, WT, DTP, DOC, and TIC could explain more than 25% of the total variations of N_2O concentrations, respectively (**Supplementary Figure S5**), acting as good predictors, while, NH_4^+, TP, TOC, PO_4^{3-}, and conductivity contributed to poor explanations for the total variations of N_2O concentrations despite the significant correlation ($p < 0.05$). When we divided the whole basin into rivers, reservoirs, and released water sections, only WT was positively correlated with N_2O concentrations in all the three types sections (**Figure 5**). For all reservoirs, *Chl-a* contributed to 37% of the total variations of N_2O concentrations (**Supplementary Figure S5**) and was a powerful influencer. DOC, TOC, and *Chl-a* were closer to N_2O concentrations in

TABLE 3 | Models of the stepwise multiple regression of ln-transformed N_2O concentrations with water environmental parameters in the river-reservoir-released water system in the Wubu River basin.

Section	Multiple linear regression model (MLR model)	R^2	*p*	Df
River	CN_2O = -6.16 + 2.41WT + 0.94DTP - 0.60PO_4^{3-}	0.572	0.004	36
Reservoirs	CN_2O = -4.93 + 0.25*Chl-a* + 1.32WT + 0.97DTP	0.577	0.008	32
Released water	CN_2O = -10.32 + 0.38 DOC + 2.77WT + 2.39DO	0.643	0.002	32
All	CN_2O = -7.49 + 2.13WT + 0.75DTP + 1.17DO - 0.33TIC	0.562	<0.001	100

"*All*" means data from the river, reservoirs, and released water sections. Nonnormally distributed candidates are ln-transformed before entering into the models

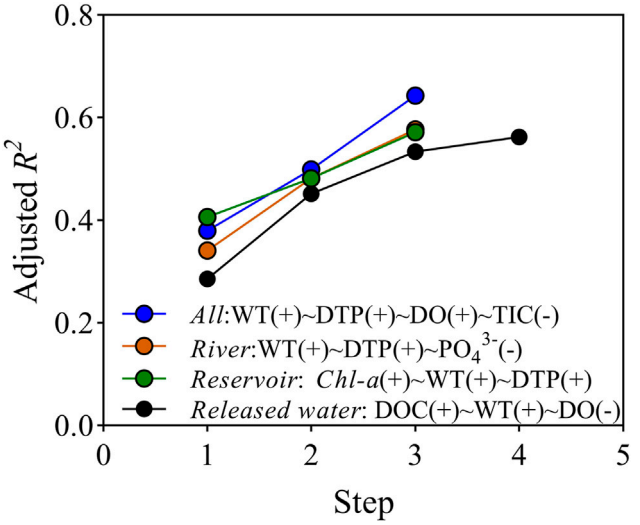

FIGURE 6 | The dynamics of adjusted R^2 for stepwise multiple regression analysis with N_2O concentrations as the dependent variables. For different models, the predictors are shown in the figure with "+" and "–" in the brackets denoting positive and negative relationships.

released water sections with the determination coefficient R^2 being 0.42, 0.39, and 0.39, respectively (**Supplementary Figure S5**). However, all variables including C, N, and P in all river sections had no significant correlation with their N_2O concentrations (**Figure 5**). Then, the results of multiple linear regressions (MLR) showed that the multipredictor models are able to resolve 57, 58, and 64% of N_2O concentrations variance for river, reservoir, and released water sections and resolve 56% of that for the whole basin (**Table 3**). There were different dominant factors affecting the N_2O concentrations in rivers, reservoirs, and released water sections, but the WT was included in all the MLR models and DTP was included in three models (**Figure 6**). Meanwhile, *Chl-a* and DOC were the first predictor of models for N_2O concentrations in reservoir and released water sections, respectively (**Figure 6**).

Furthermore, the annual N_2O fluxes showed significantly positive relations with soluble P and organic carbon, which can contribute at least 30% of the total variance of annual N_2O fluxes (**Supplementary Figure S6**). Therefore, soluble P and organic carbon can act as good predictors for the N_2O fluxes in cascaded river-reservoir systems.

Hydrologic Control on the N_2O Fluxes

In our study, the capacity of eight reservoirs was so small that the hydraulic residence time was only 0.5–3.8 days. The hydraulic residence time was found to have a significantly positive correlation with the annual average N_2O concentrations and fluxes from the cascade reservoirs in the Wubu River basin. Hydraulic residence time explained 68 and 57% variations of N_2O concentrations and fluxes in eight selected reservoirs ($p < 0.05$, **Figure 7**). Furthermore, hydraulic load (the ratio of the mean water depth to the residence time of reservoir), which regulated the vertical distribution of DO and the nutrients processing time, showed obviously negative correlation with N_2O concentrations and fluxes (**Figure 7**), with explanatory power of 47% ($p = 0.05$) and 54% ($p < 0.05$). Hydraulic residence time and hydraulic load are thus considered as good indicators for predicting the N_2O emission hotspot in these small cascade reservoirs.

DISCUSSION

The Spatial Patterns of N_2O in Cascade Damming River

River damming markedly influenced the distribution and transportation of carbon, nitrogen, and phosphorus as well as related biogeochemical processes through physical intercept and hydraulic retention time altering (Maeck et al., 2013; Shi et al., 2020). In this study, the concentrations of C, N, and P variables in the surface water of the Wubu River showed a gradual increase from upstream river-reservoir systems to the downstream ones (**Supplementary Figure S3**). The downstream reservoirs of three tributaries also were featured by higher C, N, and P concentrations. This was attributed to the fact that river damming can trap suspended particles and subsequently expedite dissolved N and P releasing accumulation along the flow direction (Liu et al., 2009a). It has been proved that the sedimentation in upstream reservoirs could be decomposed anaerobically and then discharged as dissolved N and P to downstream ones through released water, resulting in the accumulation of more bioavailable nutriments along cascaded reservoirs (Chen et al., 2020). Furthermore, hydraulic retention time has been suggested as an important governor for nutrients retention and processing in different cascaded reservoirs (Lu et al., 2016; Liang et al., 2019). In our study, the hydraulic retention time of selected reservoirs was universally short, thus having no

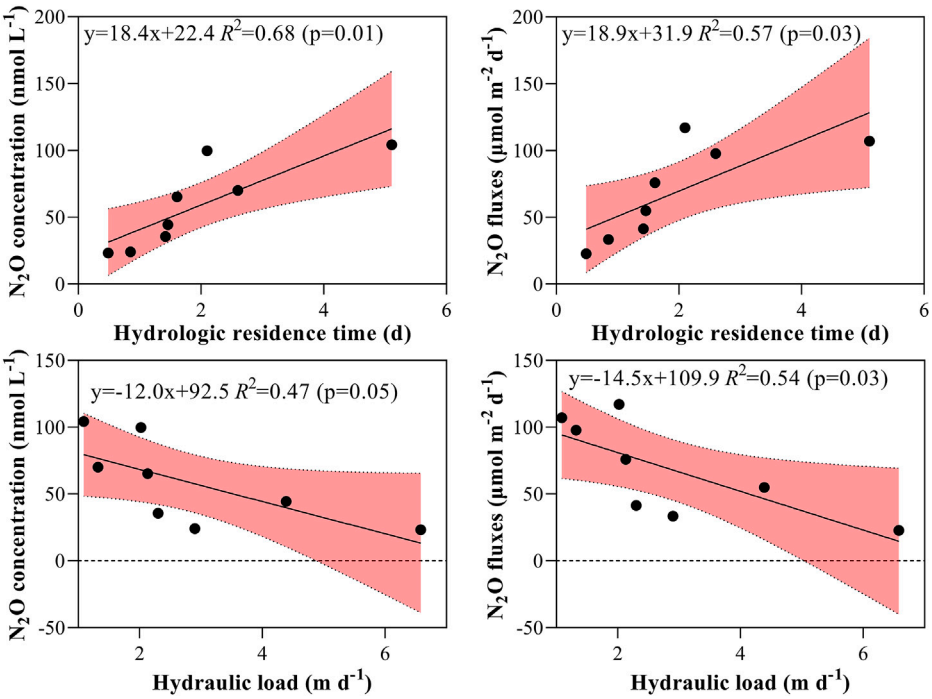

FIGURE 7 | Predictive relationships of annual averaged N_2O concentrations and fluxes with hydraulic residence time and hydraulic load of cascade reservoirs in the Wubu River basin. The translucent red shaded area means a 95% confidence interval.

significant relationship with nutrients in surface water (**Supplementary Table S5**). However, there was obviously a longer hydraulic retention time in downstream reservoirs (R4, R5, and R6), which accorded with the higher downstream C and P concentrations (**Table 1** and **Table 2**; **Supplementary Figure S7**). The accumulative effect of nutrients in surface water from upstream to downstream combined with the regulation of hydraulic retention time controlled the longitudinal variations of C, N, and P along the Wubu River.

In a single river-reservoir-released water system, in addition, C and N contents in reservoir and released water were slightly higher than those in their inflowing river, which was in accord with that from cascade reservoirs in the Lancang-Mekong River (Wu et al., 2020). It thus generated local differences in water environment parameters along the whole cascaded river-reservoir systems. Furthermore, the impounding reaches would be beneficial to algae blooms and *in situ* primary production enhancement with increasing water retention time and water depth (Liu et al., 2016). In our study, generally higher *Chl-a* in reservoir sections were indeed found than those in inflowing river sections, especially in spring and autumn (**Figure 2**). And then, the algae growth and inorganic carbon fixation would be responsible for high TOC and DOC in surface water of reservoirs (Banaszuk and Wysocka-Czubaszek, 2001; Hayer et al., 2013). We further found a significantly positive correlativity between *Chl-a* and organic carbon (**Supplementary Table S5**; **Supplementary Figure S8**). Hence, dam construction might cause nutrients redistribution and create a series of hotspots of cascaded autotrophic activity, potentially influencing the nitrogen metabolism process and the production, consumption, and emission of N_2O in rivers.

In this study, we provided a more comprehensive view of distribution patterns of the N_2O concentrations along the cascaded river-reservoir system. It resulted that N_2O concentrations exhibited remarkably longitudinal variations along the cascaded reservoirs, and the downstream reservoirs had much higher levels than the upstream ones (**Figure 3A**). The longitudinal pattern of N_2O concentrations in this smaller river basin (with a watershed area of 856 km^2) was consistent with previous studies in large river basins, such as the Lancang River (Shi et al., 2020; Wu et al., 2020) and the Wujiang River (Liang et al., 2019). Riverine N_2O, mainly derived from coupled nitrification-denitrification and denitrification, is controlled by a variety of geochemical, hydrological, and biological factors (Beaulieu et al., 2007; Beaulieu et al., 2015). On the one hand, the cascaded accumulations of dissolved inorganic nitrogen and DOC along the Wubu River (**Table 2**), which act as substrate and electron donor respectively in the denitrification process, supported high N_2O generation in downstream reservoirs (**Figure 3A**). Previous studies in cascaded river-reservoir systems suggested that dissolved N and fine particle organic matter in the sediment of downstream reservoirs were higher than the upstream ones, resulting in high denitrifying bacteria abundance and N_2O emissions (Liu et al., 2011a; Beaulieu et al., 2014; Beaulieu et al., 2015; Liu et al., 2017; Shi et al., 2017; Shi et al., 2020). On the other hand, it is well known that hydraulic residence time could govern N processing time and gaseous N emissions in rivers (Hohener and Gachter, 1993; Harrison et al.,

2008; Alexander et al., 2009) and that the long hydrological residence time allowed bacteria to settle down and to drive nitrogen mineralization and decomposition (Wang et al., 2018a; Chen et al., 2020; Deng et al., 2020). Thus, the hydraulic residence time and related hydrologic load have been considered as the important factors driving the variations of N_2O concentrations in cascade reservoirs (Liang et al., 2019; Shi et al., 2020; Yang et al., 2020). In this study, the N_2O concentrations and fluxes were found to be positively correlated with hydraulic residence time and negative with hydraulic load significantly (**Figure 7**), implying the regulating and controlling of hydrological conditions on the spatial variations of N_2O emissions in the Wubu River cascaded reservoirs. Furthermore, in our investigation, the dissolved N_2O in surface water may be mainly derived from deep waters and sediments because of the denitrification limitation by generally high DO in the water column (**Table 2**). The increase in water depth in downstream reservoirs (**Table 1**) created an anoxic advantage and opportunity for denitrification in sediments and favored the accumulation of dissolved N_2O in water. The significantly higher N_2O concentrations in released waters from the bottom of reservoirs fed the downstream reaches and formed accumulation in downstream reservoirs (Cheng et al., 2019; Wu et al., 2020). Hence, alternant impounding along the Wubu River could create a serial N_2O energizer and increase the holistic N_2O emissions.

We further explored the local variation patterns of N_2O concentrations in individual "river-reservoir-released water" system in the Wubu River basin (**Figure 3A**). It was certain that impoundment-affected reaches could provide favorable conditions for N_2O production and accumulation *via* interception of bioavailability nutrients, anaerobic environment of deepened water, and increase of hydraulic retention time (Beaulieu et al., 2015; Liang et al., 2019). Thus, N_2O concentrations in impounding reaches were much higher (**Figure 3A**), amounting 1.2–7.9 (2.7) times these in their upstream channels. Meanwhile, released water from the bottom of reservoirs had exceptionally high N_2O concentrations, approximately 1.3–12.2 (3.4) times the upstream channels. Thus, N_2O concentrations presented a common pattern of "low upstream channel, high reservoir, and higher released water" across the cascaded "river-reservoir-released water" systems. Such pattern of N_2O concentrations was consistent with previous reports in other single or cascaded river-reservoir systems (Liu et al., 2009b; Liu et al., 2011a; Liu et al., 2017; Cheng et al., 2019). For example, Yang et al. (2020) found that the N_2O emissions in the impoundment-affected Huoshaogou River were much higher than the upper rivers as influenced by enrichment of N and OC in sediment after river damming. Liu et al. (2017) also found that the N_2O emission fluxes in released water sections were five times higher than those in reservoir sections in Dongfeng Reservoirs. In addition, the obvious N_2O loss between the released water sections and the following river sections (**Figure 3A**) suggested potential massive N_2O evasions from similar sections along the Wubu River basin. A study by Liu et al. (2009b) in the cascaded damming Maotiao River also found that N_2O concentrations in the river sections were significantly lower than the upstream released water sections, while they increased again in the next reservoir sections. It was suggested that the cascaded impounding and releasing would create novel N_2O emission hotspots along the river (Liu et al., 2009b; Yang et al., 2020), which enhanced the uncertainty of the total estimation of N_2O emissions from rivers, and that continuous dams caused an amplifying effect on surface water N_2O emissions from rivers. As the end result, the N_2O concentrations and emissions presented more complicated spatial patterns coupling of "gradual increase trend from upstream to downstream" and "low river-high reservoir-higher released water" in the whole Wubu River cascade dam systems.

Seasonal Variation of N_2O Concentrations and Its Potential Control

The seasonal variations of N_2O concentrations in the Wubu River basin showed the highest in autumn and the lowest in winter (**Figure 3B**). It presented a similar seasonal pattern to previous studies (Cole and Caraco, 2001; Burgos et al., 2015). The seasonal variations of riverine N_2O concentrations have been suggested to be mainly controlled by the seasonal temperature, precipitation, and runoff inflowing (Beaulieu et al., 2007; Outram and Hiscock, 2012; Freymond et al., 2013). High temperature in freshwater is generally regarded as the primary reason for high N_2O concentrations in the warm season on account of stimulating *in situ* microbial activity (Zhu et al., 2013; Beaulieu et al., 2015; Wang et al., 2017b). Silvennoinen et al. (2008b) found that the riverine N_2O emissions were strongly sensitive to temperature as a result of the regulations on the abundance and activity of denitrifying bacteria. Previous studies also confirmed the prominent temperature sensitivity of denitrification in aquatic systems (Smensen et al., 1988; Beaulieu et al., 2011; Bouletreau et al., 2012). Zhou et al. (2016) found the N_2O emissions with increasing temperatures in Jiulong cascade reservoirs. In our study, the WT had a significantly positive correlation with N_2O concentrations (**Figure 5**) and was included in all the MLR models as pivotal predictors for N_2O variations (**Figure 6**). In addition, rainfall was another factor influencing the seasonal pattern of dissolved N_2O concentrations in rivers (Outram and Hiscock, 2012) *via* directly increasing N_2O input from terrestrial soils or indirectly enhancing allochthonous organic matter input to fuel *in situ* denitrification (Beaulieu et al., 2012; Wang et al., 2017b). Meanwhile, heavy rainfall would lead to a rapid increase in river flow and then a dilution effect on dissolved N_2O concentrations in surface water (Wang et al., 2017b). The lower N_2O concentrations in summer, despite the high temperature, could be attributed to the dilution effect as a result of continuous rainfall during the investigating period (Wang et al., 2017b). Therefore, the combined effect of temperature and rainfall dilution has determined the seasonal variations of N_2O concentrations in the Wubu River.

In addition, we further found that the seasonal patterns of N_2O concentrations in flowing river sections were consistent with those in static reservoirs for "river-reservoir-released water"

systems, indicating that cascaded damming would not alter the seasonal pattern of N_2O concentrations in the Wubu River. However, the amplitudes of seasonal N_2O variations in reservoirs and released waters were much higher than those in inflowing river sections (**Figure 3B**), implying that the damming enhanced the seasonal variations of riverine N_2O concentrations. The spatial variations of dissolved N_2O concentrations in river sections and reservoirs were significantly affected by their seasonality (**Supplementary Figure S4**). The amplitudes of N_2O spatial variations were found to be the most significant in spring and autumn but were almost absent in winter. Particularly, N_2O spatial variations were so minor in summer owing to frequent rainfall and rapidly hydrological mixing of the upper and lower reaches. Investigations with high spatiotemporal resolution are needed to promote the understanding of N_2O emissions in fragmentation habitat caused by river damming.

Potential Controls on N_2O Emissions in the Cascade River-Reservoir Systems

The spatial heterogeneity of N_2O concentrations existed in the cascaded river-reservoir systems and was closely related to water physicochemical properties (**Figure 4A**). N_2O is well known to be derived from nitrification and denitrification, and oxygen and nitrogen availability have been reported to be important factors controlling the N_2O producing processes (Beaulieu et al., 2011; Hinshaw and Dahlgren, 2013; Liang et al., 2019). In this study, however, there was no clear relationship between the N_2O with DO, TN, and NO_3^-, disobeying the results of previous studies (Beaulieu et al., 2014; Cheng et al., 2019; Liang et al., 2019). DO in water column were relatively high in the whole Wubu River basin (**Table 2**). Meanwhile, short hydraulic retention time and shallow water promote vertical mixing of DO in the water profile and limit N_2O production by nitrification pathway in water column (Beaulieu et al., 2014; Liang et al., 2019). Poor correlations of N_2O concentrations with NO_3^- (**Supplementary Figure S5**) supported the viewpoint that denitrification in oxygen-rich water would contribute to insignificant N_2O (Beaulieu et al., 2014; Beaulieu et al., 2015), while the significant relationship between N_2O concentrations and NH_4^+ implied the coupling nitrification-denitrification process (i.e., intermediate products in nitrification participate in denitrification process) in the water column which acted as possible sources of N_2O production (Rosamond et al., 2011; Beaulieu et al., 2015). Previous studies in freshwater or culture pond found that the N_2O production processes could be influenced by NH_4^+ due to the coupling nitrification-denitrification (Mao et al., 2005; Beaulieu et al., 2015; Yang and Tong, 2015; Liu et al., 2019). However, NH_4^+ concentrations could only play a poor indicator for N_2O concentrations explaining 17% of the overall variances (**Supplementary Figure S5**), indicating that the contribution of coupling nitrification-denitrification process to N_2O concentrations in oxygen-rich water column was limited. Despite high DO concentrations in surface water, previous studies showed that microbial respiration in overlying water could develop anaerobic conditions when water depth exceeding 2–5 m, resulting in the occurrence of denitrification at sediment layers (Wenk et al., 2016). In our study, cascaded damming increased averaged depth in reservoirs and thus raised the opportunity and duration for denitrification in sediment, improving the N_2O production.

In the present study, the P (including TP, DTP, and PO_4^{3-}) and C (DOC and TOC) were significantly and positively correlated with the N_2O concentrations (**Figure 4**). Extremely low C:N (6.7 ± 2.8) and high N:P (35 ± 13) in the Wubu River indicated that organic carbon and phosphorus concentrations would dominate biologically driven nitrification and denitrification (**Table 2**). Mehnaz and Dijkstra (2016) found that P availability and aerobic metabolism caused hypoxia in water benefiting high N_2O production. Liu and Song (2009) showed that P could stimulate N cycling and strengthen nitrification and denitrification in freshwater marsh. DTP was included in multi-MLR models in our study (**Table 3**; **Figure 6**). Meanwhile, organic carbon, as important material substrates for microbial metabolism and *in situ* respiration in river water, could affect the oxygen consumption rates and subsequently form anaerobic conditions (Nirmal Rajkumar et al., 2008), in turn, favoring the N_2O producing processes. MLR suggested that DOC was the first predictor of models for N_2O concentrations in released waters draining from the bottom of reservoirs (**Figure 6**). It indicated that OC could affect the N_2O production from the deep water and sediment in reservoirs. Thus, the accumulation of P and C in the bottom of the cascaded reservoirs may be important mechanisms for the local pattern of N_2O fluxes in individual "river-reservoir-released water" system.

Interestingly, the N_2O concentrations had a positive correlation with *Chl-a* in reservoirs and released waters. *Chl-a* concentrations can explain 37–39% of the N_2O variations among different reservoir sections and released water sections (**Supplementary Figure S5**). *Chl-a* plays the first predictor for N_2O concentrations variance in reservoirs (**Figure 6**). It indicated that algae blooms and enhanced primary production in surface water as a result of dam impoundment could enhance riverine N_2O production, similar to other studies in eutrophic rivers or reservoirs (Mao et al., 2005; Wang et al., 2017a). This may be attributed to the fact that algae blooms could supply fresh organic matter when algae die and enhance anaerobic conditions of deep water (Feng et al., 2016). Thus, cascaded damming in rivers would create a series of hotspots of eutrophication along the flow direction and then develop a continuous actuator of N_2O production.

In addition to water environmental factors, we highlighted the importance of hydrologic conditions alteration dominating N biogeochemical cycle and N_2O variation among cascaded reservoirs in the Wubu River (**Figure 7**). Similar to other studies in large rivers (Wang et al., 2018b; Liang et al., 2019), our results also showed a significant correlation of N_2O fluxes with hydraulic residence time in the cascade reservoirs. The hydraulic load was found to have significant negative correlations with N_2O concentrations and fluxes, consistent with a study in the Wujiang cascade reservoirs (Liang et al., 2019). On the one hand, the hydraulic residence time and water depth could regulate the DO vertical mixing in the water profile

TABLE 4 | Comparison of N_2O fluxes with other water bodies worldwide.

River	Climate	FN_2O ($\mu mol \cdot m^{-2} \cdot d^{-1}$)	N_2O concentration ($nmol \cdot L^{-1}$)	k_0 ($cm\ h^{-1}$)	Method	References
Stream of Yangtze River	Plateau	1.1–5.9	—	27.1–34.2	Diffusion model	Qu et al. (2017)
Stream of Yellow River	Plateau	1.8–50.9	—	15.0–117.1	—	—
Temmesjoki River	Frigid	−10.4–65.9	6.7–47	40.4–54.2	floating static chambers	Silvennoinen et al. (2008a)
Ohio River	Temperate	8.9–339.7	—	—	Floating chambers	Beaulieu et al. (2010)
Guadalete River	Temperate	−0.1–313.2	9.7–265.3	—	Wind speed model	Burgos et al. (2015)
San Joaquin River	Mediterranean	5.2–202.8 14.3–112.9	0.007–0.04	—	Floating chambers, based model	Hinshaw and Dahlgren, (2013)
Québec River	Temperate	−23.1–16.9	-4.3–8.7	0.0–52.9	Based on model	Soued et al. (2015)
Neuse River watersged	Subtropical	−5.0–35.4	—	—	Floating chambers	Stow et al. (2005)
The upper Mekong River	Subtropical	0.3–0.6	—	—	The boundary-layer model	(Liang et al., 2019; Shi et al., 2020)
Wujiang River	Subtropical	−7.9–337.2	4.0–447.2	—	The boundary-layer model	Liang et al. (2019)
Jiulong River	Subtropical	37.8	27.0	—	Floating chambers	Chen et al. (2015)
Yangtze River	Subtropical	1.0–22.2	7.7–16.4	5.8–7.1	Wind speed-hydrologic model	Yan et al. (2012)
Simunjan	Tropical	−0.005–0.04	3.8–34.0	—	Based on model	Bange et al. (2019)
Rajang	Tropical	−0.008–0.03	4.0–19.1	—	—	—
Global rivers	—	—	12.1	—	—	Soued et al. (2015)
Three Gorges Reservoir	Subtropical	−2.5–44.6	7.6 ± 11.5	—	Floating chambers	Zhu et al. (2013)
Hongjiadu reservoir	Subtropical	2.4–31.7	16.4–44.1	—	The boundary-layer model	Liu et al. (2011a)
Wujiangdu reservoir	—	1.9–42.2	16.5–74.7	—	—	—
Miyun reservoir	Temperate	−1.2–99.5	—	—	Static chambers	Yang et al. (2015)
MoChou	Frigid	1.69 ± 3.7	—	—	Static chambers	Liu et al. (2011b)
TuanJie	—	1.36 ± 1.5	—	—	—	—
Daming	—	3.93 ± 3.8	—	—	—	—
China reservoirs	—	23.09 ± 32.57	—	—	—	Li et al. (2018)
Global reservoirs	—	6.82	—	—	—	Deemer et al. (2016)
Wubu River	—	−11.8–805.6	2.5–283.2	—	—	—
Upstream R1–R3	Subtropical	−0.2–194.9	6.8–75.5	4.4–17.2	Wind speed-hydrologic model	This study
Downstream R4–R8	—	23.1–805.6	16.8–283.2	—	—	—

and nitrification, denitrification in deep waters and sediments (Wenk et al., 2016), and then control the N_2O emissions from reservoirs. On the one hand, C, N, and P retention and processing time are influenced by the hydraulic retention time (Saunders and Kalff, 2001; Cook et al., 2009; Wang, 2020), thereby regulating the N biogeochemical cycle. Hydraulic residence time can also govern N_2O production in reservoirs by promoting nutrients mineralization and release and consequent eutrophication (Beaulieu et al., 2015; Wenk et al., 2016). In this study, longer hydraulic residence time and smaller hydraulic load in the downstream reservoirs (**Table 1**) were important drivers for the spatial variations of N_2O concentrations in the Wubu River cascade reservoirs. Our results suggested that hydraulic conditions as a prerequisite for regulating N removal and gaseous N emissions could predict the variation pattern of N_2O fluxes in this small river basin.

N_2O Fluxes Compared With Other Studies

k_0 in this study ranged from 4.4 to 17.2 $cm\ h^{-1}$, similar to other studies, e.g., tributaries of the Yangtze River (Qu et al., 2017), Temmesjoki River (Silvennoinen et al., 2008a), and Québec River (Soued et al., 2015). There were significantly higher k_0 values for the inflowing river sections and released water sections than these for reservoir sections due to low turbulence in impounded reaches. Based on the boundary-layer model and conservative k_0 (Borges et al., 2004), the calculated N_2O fluxes for the Wubu River basin ranged from −11.8 to 805.6 $\mu mol\ m^{-2} \cdot d^{-1}$ with an overall mean of 104.6 ± 98.4 $\mu mol\ m^{-2} \cdot d^{-1}$. The amplitude of N_2O fluxes variation in the Wubu River exceeded three orders, showing disproportionately strong variations given its small river basin compared with other studies in large rivers (Beaulieu et al., 2010; Yan et al., 2012; Chen et al., 2015). The strong variations of N_2O fluxes have also been found in the Maotiao River, Mekong River, and other cascaded damming rivers in subtropics (Liang et al., 2019; Shi et al., 2020). The amplitude of N_2O fluxes variations in the Wubu River was higher than those from the river network in Québec, the upper Mekong River, and Yangtze River, which had a significantly large catchment area (Yan et al., 2012; Soued et al., 2015; Shi et al., 2020). Those variations were attributed to habitat fragmentation and "river-reservoir" alternate systems with different hydraulic loads (Liang et al., 2019). Hence, cascade damming might cause more complicated spatial heterogeneity for riverine N_2O emissions.

Meanwhile, the averaged N_2O fluxes in the Wubu River basin were relatively higher compared with other studies worldwide (**Table 4**), although significantly lower N_2O emission fluxes were

found in upstream river-reservoir systems (**Figure 4A**). The N_2O fluxes in the Wubu River basin were significantly higher than those in natural rivers, such as the tributaries of the Yangtze River and Yellow River (Qu et al., 2017) and Neuse River (Stow et al., 2005) and higher than these in some subtropical, temperate, and cold reservoirs (**Table 4**). The N_2O fluxes in our study were even higher than some contaminated rivers located in urban and agricultural areas (Beaulieu et al., 2010; Hinshaw and Dahlgren, 2013). At the same time, the N_2O fluxes in the eight small reservoirs were three times and 10 times higher than the average values of China's reservoirs and global reservoirs, respectively (Deemer et al., 2016; Li et al., 2018). Meanwhile, the N_2O fluxes in upstream river-reservoir sections were comparable to those in the natural Guadalete River (Burgos et al., 2015) and San Joaquin River (Hinshaw and Dahlgren, 2013). In addition, N_2O fluxes from all reservoir sections and released water sections were much higher than those from inflowing river sections, indicating that cascaded dams can enhance the whole N_2O emissions level from the fluvial continuum. Thus, continuous dams were regarded as one of the important factors controlling N_2O emissions in rivers, and more research should be done to quantify the contribution of cascade damming to riverine N_2O budgets.

CONCLUSION

This study focused on the spatiotemporal patterns in N_2O concentrations and emissions from a cascade damming with a small river basin and the local variations of N_2O emissions among the inflowing river, reservoir, and released water sections. The results demonstrated that the Wubu River basin served as a strong source of atmospheric N_2O under cascade damming. The N_2O concentrations and emissions exhibited obvious increase trends along the flow direction, and downstream reservoirs aced as hotspots of N_2O emissions. All reservoir sections and their released water had higher N_2O concentrations than their upstream inflowing river sections, presenting a generally local pattern of N_2O emissions with "low river-high reservoir-extremely high released water." Cascaded reservoirs and released water sections acted as "reactors" of N_2O production along the Wubu River, significantly amplifying the riverine N_2O emissions. *Chl-a*, organic carbon, and soluble phosphorus concentrations were indicated as dominant factors regulating the N_2O concentrations. The N_2O concentrations and fluxes in reservoirs had a significant correlation with hydraulic residence time and hydraulic load, suggesting hydrologic conditions alteration dominate N_2O variations among cascaded reservoirs in the Wubu River. Seasonal variations of N_2O concentrations and fluxes were mainly controlled by temperature and rainfall. It was highlighted that the cascade reservoirs not only acted as exciters for N_2O production and emissions but also formed cumulative effects and local hotspots along the longitudinal dimension, significantly increasing the complexity of the spatiotemporal variability in riverine N_2O emissions.

DATA AVAILABILITY STATEMENT

The raw data supporting the conclusions of this article will be made available by the authors, without undue reservation.

AUTHOR CONTRIBUTIONS

XY: conceptualization, methodology, and supervision. YH: investigation and validation. XW and SW: investigation, data curation, and writing—reviewing and editing. TL, JW, HL, ZQ, LY, and YZ: visualization.

FUNDING

This research was financially supported by the National Natural Science Foundation of China (No. 41807321), Chongqing Basic Research and Frontier Exploration Foundation (No. cstc2018jcyjAX0672), Science and Technology Research Program of Chongqing Education Commission of China (Nos. KJQN201800530 and KJZD-K202000502), and Sichuan Science and Technology Project (No. 2021YFS0286).

SUPPLEMENTARY MATERIAL

The Supplementary Material for this article can be found online at: https://www.frontiersin.org/articles/10.3389/fenvs.2021.728489/full#supplementary-material

REFERENCES

Akbarzadeh, Z., Maavara, T., Slowinski, S., and Van Cappellen, P. (2019). Effects of Damming on River Nitrogen Fluxes: A Global Analysis. *Glob. Biogeochem. Cycles* 33 (11), 1339–1357. doi:10.1029/2019gb006222

Alexander, L. V., Allen, S. K., Bindoff, N. L., Bréon, F.-M., Church, J. A., Cubasch, U., et al. (2013). *Summary for Policymakers:Climate Change 2013:The Physical Science Basis, in Contribution of Working Group I (WGI) to the Fifth Assessment Report (AR5) of the Intergovernmental Panel on Climate Change (IPCC).* Cambridge, United Kingdom and New York, NY, USA: Cambridge University Press.

Alexander, R. B., Böhlke, J. K., Boyer, E. W., David, M. B., Harvey, J. W., Mulholland, P. J., et al. (2009). Dynamic Modeling of Nitrogen Losses in River Networks Unravels the Coupled Effects of Hydrological and Biogeochemical Processes. *Biogeochemistry* 93 (1-2), 91–116. doi:10.1007/s10533-008-9274-8

Bala, G., Bopp, L., Brovkin, V., Canadell, J., Chhabra, A., DeFries, R., IPCC, et al. (2013). in *Working Group I Contribution to the IPCC Fifth Assessment Report Climate Change 2013:the Physical Science Basis*. Editor I. P. O.C.C (New York: Cambridge University Press).

Banaszuk, P., and Wysocka-Czubaszek, A. (2001). *The Role of Natural Biogeochemical Barriers in Protection of Surface Waters against Eutrophication*.

Bange, H. W., Sim, C. H., Bastian, D., Kallert, J., Kock, A., Mujahid, A., et al. (2019). Nitrous Oxide (N2O) and Methane (CH4) in Rivers and Estuaries of

Northwestern Borneo. *Biogeosciences* 16 (22), 4321–4335. doi:10.5194/bg-16-4321-2019

Beaulieu, J. J., Arango, C. P., Hamilton, S. K., and Tank, J. L. (2007). The Production and Emission of Nitrous Oxide from Headwater Streams in the Midwestern United States. *Glob. Change Biol.* 14 (4), 878–894. doi:10.1111/j.1365-2486.2007.01485.x

Beaulieu, J. J., Nietch, C. T., and Young, J. L. (2015). Controls on Nitrous Oxide Production and Consumption in Reservoirs of the Ohio River Basin. *J. Geophys. Res. Biogeosci.* 120 (10), 1995–2010. doi:10.1002/2015jg002941

Beaulieu, J. J., Shuster, W. D., and Rebholz, J. A. (2012). Controls on Gas Transfer Velocities in a Large River. *J. Geophys. Res.* 117 (G2), a–n. doi:10.1029/2011jg001794

Beaulieu, J. J., Shuster, W. D., and Rebholz, J. A. (2010). Nitrous Oxide Emissions from a Large, Impounded River: The Ohio River. *Environ. Sci. Technol.* 44 (19), 7527–7533. doi:10.1021/es1016735

Beaulieu, J. J., Smolenski, R. L., Nietch, C. T., Townsend-Small, A., Elovitz, M. S., and Schubauer-Berigan, J. P. (2014). Denitrification Alternates between a Source and Sink of Nitrous Oxide in the Hypolimnion of a Thermally Stratified Reservoir. *Limnol. Oceanogr.* 59 (2), 495–506. doi:10.4319/lo.2014.59.2.0495

Beaulieu, J. J., Tank, J. L., Hamilton, S. K., Wollheim, W. M., Hall, R. O., Mulholland, P. J., et al. (2011). Nitrous Oxide Emission from Denitrification in Stream and River Networks. *Proc. Natl. Acad. Sci. USA*. 108 (1), 214–219. doi:10.1073/pnas.1011464108

Beusen, A. H. W., Bouwman, A. F., Van Beek, L. P. H., Mogollón, J. M., and Middelburg, J. J. (2016). Global Riverine N and P Transport to Ocean Increased during the 20th century Despite Increased Retention along the Aquatic Continuum. *Biogeosciences* 13 (8), 2441–2451. doi:10.5194/bg-13-2441-2016

Borges, A. V., Vanderborght, J.-P., Schiettecatte, L.-S., Gazeau, F., Ferrón-Smith, S., Delille, B., et al. (2004). Variability of the Gas Transfer Velocity of CO2 in a Macrotidal Estuary (The Scheldt). *Estuaries* 27 (4), 593–603. doi:10.1007/BF02907647

Boulêtreau, S., Salvo, E., Lyautey, E., Mastrorillo, S., and Garabetian, F. (2012). Temperature Dependence of Denitrification in Phototrophic River Biofilms. *Sci. Total Environ.* 416, 323–328. doi:10.1016/j.scitotenv.2011.11.066

Boyer, E. W., Howarth, R. W., Galloway, J. N., Dentener, F. J., Green, P. A., and Vörösmarty, C. J. (2006). Riverine Nitrogen export from the Continents to the Coasts. *Glob. Biogeochem. Cycles* 20 (1), a–n. doi:10.1029/2005gb002537

Burgos, M., Sierra, A., Ortega, T., and Forja, J. M. (2015). Anthropogenic Effects on Greenhouse Gas (CH4 and N2O) Emissions in the Guadalete River Estuary (SW Spain). *Sci. Total Environ.* 503-504, 179–189. doi:10.1016/j.scitotenv.2014.06.038

Chang, X., Liu, X., and Zhou, W. (2010). Hydropower in China at Present and its Further Development. *Energy* 35 (11), 4400–4406. doi:10.1016/j.energy.2009.06.051

Chen, J., Cao, W., Cao, D., Huang, Z., and Liang, Y. (2015). Nitrogen Loading and Nitrous Oxide Emissions from a River with Multiple Hydroelectric Reservoirs. *Bull. Environ. Contam. Toxicol.* 94 (5), 633–639. doi:10.1007/s00128-015-1525-5

Chen, Q., Shi, W., Huisman, J., Maberly, S. C., Zhang, J., Yu, J., et al. (2020). Hydropower Reservoirs on the Upper Mekong River Modify Nutrient Bioavailability Downstream. *Natl. Sci. Rev.* 7 (9), 1449–1457. doi:10.1093/nsr/nwaa026

Cheng, F., Zhang, H.-M., Zhang, G.-L., Liu, S.-M., Song, G.-D., and Du, G.-X. (2019). Distribution and Emission of N2O in the Largest River-Reservoir System along the Yellow River. *Sci. Total Environ.* 666, 1209–1219. doi:10.1016/j.scitotenv.2019.02.277

China's State Environmental Protection (2002). *Monitoring and Analysis Method of Water and Waste Water*. Beijing: Chinese Environment Science Press.

Clough, T. J., Buckthought, L. E., Kelliher, F. M., and Sherlock, R. R. (2007). Diurnal Fluctuations of Dissolved Nitrous Oxide (N2O) Concentrations and Estimates of N2O Emissions from a spring-fed River: Implications for IPCC Methodology. *Glob. Change Biol.* 13 (5), 1016–1027. doi:10.1111/j.1365-2486.2007.01337.x

Cole, J. J., and Caraco, N. F. (2001). Emissions of Nitrous Oxide (N2O) from a Tidal, Freshwater River, the Hudson River, New York. *Environ. Sci. Technol.* 35 (6), 991–996. doi:10.1021/es0015848

Cook, P. L. M., Aldridge, K. T., Lamontagne, S., and Brookes, J. D. (2009). Retention of Nitrogen, Phosphorus and Silicon in a Large Semi-arid Riverine lake System. *Biogeochemistry* 99 (1-3), 49–63. doi:10.1007/s10533-009-9389-6

Deemer, B. R., Harrison, J. A., Li, S., Beaulieu, J. J., DelSontro, T., Barros, N., et al. (2016). Greenhouse Gas Emissions from Reservoir Water Surfaces: A New Global Synthesis. *BioScience* 66 (11), 949–964. doi:10.1093/biosci/biw117

Deng, H., Tao, Z., Gao, Q., Yao, L., Feng, Y., Li, Y., et al. (2020). Variation of Biogeochemical Cycle of Riverine Dissolved Inorganic Carbon and Silicon with the cascade Damming. *Environ. Sci. Pollut. Res.* 27 (23), 28840–28852. doi:10.1007/s11356-020-09174-5

Deyan, L., and Changchun, S. (2009). Effects of Inorganic Nitrogen and Phosphorus Enrichment on the Emission of N2O from a Freshwater Marsh Soil in Northeast China. *Environ. Earth Sci.* 60 (4), 799–807. doi:10.1007/s12665-009-0217-z

Feng, W. Y., Zhu, Y. R., Wu, F. C., Zhang, X., and Zhang, C. (2016). The Fluorescent Characteristics and Sources of Dissolved Organic Matter in Water of Tai Lake, China. *Acta Scientiae Circumstantiae* 36 (2), 475–482. doi:10.13671/j.hjkxxb.2015.0652

Freymond, C. V., Wenk, C. B., Frame, C. H., and Lehmann, M. F. (2013). Year-round N2O Production by Benthic NOx Reduction in a Monomictic South-alpine lake. *Biogeosciences* 10 (12), 8373–8383. doi:10.5194/bg-10-8373-2013

Grumbine, R. E., and Xu, J. (2011). Mekong Hydropower Development. *Science* 332 (6026), 178–179. doi:10.1126/science.1200990

Guérin, F., Abril, G., Tremblay, A., and Delmas, R. (2008). Nitrous Oxide Emissions from Tropical Hydroelectric Reservoirs. *Geophys. Res. Lett.* 35 (6), L06404. doi:10.1029/2007gl033057

Harrison, J. A., Maranger, R. J., Alexander, R. B., Giblin, A. E., Jacinthe, P.-A., Mayorga, E., et al. (2008). The Regional and Global Significance of Nitrogen Removal in Lakes and Reservoirs. *Biogeochemistry* 93 (1-2), 143–157. doi:10.1007/s10533-008-9272-x

Hayer, C. A., Holcomb, B. M., and Chipps, S. R. (2013). Associations between Iron Concentration and Productivity in Montane Streams of the Black Hills, South Dakota. *The Prairie Naturalist* 45 (3), 68–76.

He, S., Guo, S., Yang, G., Chen, K., Liu, D., and Zhou, Y. (2019). Optimizing Operation Rules of Cascade Reservoirs for Adapting Climate Change. *Water Resour. Manage.* 34 (1), 101–120. doi:10.1007/s11269-019-02405-6

He, Y., Wang, X., Chen, H., Yuan, X., Wu, N., Zhang, Y., et al. (2017b). Effect of Watershed Urbanization on N2O Emissions from the Chongqing Metropolitan River Network, China. *Atmos. Environ.* 171, 70–81. doi:10.1016/j.atmosenv.2017.09.043

Hinshaw, S. E., and Dahlgren, R. A. (2013). Dissolved Nitrous Oxide Concentrations and Fluxes from the Eutrophic San Joaquin River, California. *Environ. Sci. Technol.* 47 (3), 1313–1322. doi:10.1021/es301373h

Hohener, P., and Gachter, R. (1993). Prediction of Dissolved Inorganic Nitrogen (DIN) Concentrations in Deep, Seasonally Stratified Lakes Based on Rates of DIN Input and N Removal Processes. *Aquat. Sci.* 55 (2), 112–131. doi:10.1007/bf00877440

Jin, H., Yoon, T. K., Begum, M. S., Lee, E.-J., Oh, N.-H., Kang, N., et al. (2018). Longitudinal Discontinuities in Riverine Greenhouse Gas Dynamics Generated by Dams and Urban Wastewater. *Biogeosciences* 15 (20), 6349–6369. doi:10.5194/bg-15-6349-2018

Koschorreck, M., Prairie, Y. T., Kim, J., and Marcé, R. (2021). Technical Note: CO2 Is Not like CH4 - Limits of and Corrections to the Headspace Method to Analyse pCO2 in Fresh Water. *Biogeosciences* 18 (5), 1619–1627. doi:10.5194/bg-2020-307

Li, S., Bush, R. T., Santos, I. R., Zhang, Q., Song, K., Mao, R., et al. (2018). Large Greenhouse Gases Emissions from China's Lakes and Reservoirs. *Water Res.* 147, 13–24. doi:10.1016/j.watres.2018.09.053

Liang, X., Xing, T., Li, J., Wang, B., Wang, F., He, C., et al. (2019). Control of the Hydraulic Load on Nitrous Oxide Emissions from Cascade Reservoirs. *Environ. Sci. Technol.* 53 (20), 11745–11754. doi:10.1021/acs.est.9b03438

Liss, P. S., and Slater, P. G. (1974). Flux of Gases across the Air-Sea Interface. *Nature* 247 (5438), 181–184. doi:10.1038/247181a0

Liu, C. Q., Wang, F. S., Wamg, Y. C., and Wang, B. L. (2009a). Responses of Aquatic Environment to River Damming——from the geochemical view. *Resour. Environ. Yangtze Basin* 18 (4), 384–396. doi:10.1016/S1874-8651(10)60080-4

Liu, S., Lu, X. X., Xia, X., Zhang, S., Ran, L., Yang, X., et al. (2016). Dynamic biogeochemical controls on river *p*CO2 and recent changes under aggravating river impoundment: An example of the subtropical Yangtze River. *Glob. Biogeochem. Cycles* 30 (6), 880–897. doi:10.1002/2016gb005388

Liu, X.-L., Liu, C.-Q., Li, S.-L., Wang, F.-S., Wang, B.-L., and Wang, Z.-L. (2011a). Spatiotemporal variations of nitrous oxide (N2O) emissions from two reservoirs in SW China. *Atmos. Environ.* 45 (31), 5458–5468. doi:10.1016/j.atmosenv.2011.06.074

Liu, X., Li, S., Wang, Z., Han, G., Li, J., Wang, B., et al. (2017). Nitrous oxide (N2O) emissions from a mesotrophic reservoir on the Wujiang River, southwest China. *Acta Geochim* 36 (4), 667–679. doi:10.1007/s11631-017-0172-4

Liu, X. L., Liu, C. Q., Li, S. L., Shun, W. F., Li, W. B., Jin, G., et al. (2009b). Producing and releasing mechanism of N_2O in cascade reservoris of Maotiao River in summer. *Resour. Environ. Yangtze Basin* 18 (4), 373–378. doi:10.1016/S1874-8651(10)60080-4

Liu, Y., Zhu, R., Ma, D., Xu, H., Luo, Y., Huang, T., et al. (2011b). Temporal and spatial variations of nitrous oxide fluxes from the littoral zones of three alga-rich lakes in coastal Antarctica. *Atmos. Environ.* 45 (7), 1464–1475. doi:10.1016/j.atmosenv.2010.12.017

Lu, T., Chen, N., Duan, S., Chen, Z., and Huang, B. (2016). Hydrological controls on cascade reservoirs regulating phosphorus retention and downriver fluxes. *Environ. Sci. Pollut. Res.* 23 (23), 24166–24177. doi:10.1007/s11356-016-7397-3

Maavara, T., Lauerwald, R., Regnier, P., and Van Cappellen, P. (2017). Global perturbation of organic carbon cycling by river damming. *Nat. Commun.* 8, 15347. doi:10.1038/ncomms15347

Maavara, T., Parsons, C. T., Ridenour, C., Stojanovic, S., Dürr, H. H., Powley, H. R., et al. (2015). Global phosphorus retention by river damming. *Proc. Natl. Acad. Sci. USA* 112 (51), 15603–15608. doi:10.1073/pnas.1511797112

Maeck, A., DelSontro, T., McGinnis, D. F., Fischer, H., Flury, S., Schmidt, M., et al. (2013). Sediment Trapping by Dams Creates Methane Emission Hot Spots. *Environ. Sci. Technol.* 47 (15), 8130–8137. doi:10.1021/es4003907

Mao, Z. P., Wang, Y. C., Peng, W. Q., and Zhou, H. D. (2005). Advances in effects of dams on river ecosystem. *Adv. Water Sci.* 16 (1), 134–140. doi:10.14042/j.cnki

Mehnaz, K. R., and Dijkstra, F. A. (2016). Denitrification and associated N 2 O emissions are limited by phosphorus availability in a grassland soil. *Geoderma* 284, 34–41. doi:10.1016/j.geoderma.2016.08.011

Middelburg, J. J. (2020). Are nutrients retained by river damming. *Natl. Sci. Rev.* 7 (9), 1458. doi:10.1093/nsr/nwaa073

Nirmal Rajkumar, A., Barnes, J., Ramesh, R., Purvaja, R., and Upstill-Goddard, R. C. (2008). Methane and nitrous oxide fluxes in the polluted Adyar River and estuary, SE India. *Mar. Pollut. Bull.* 56 (12), 2043–2051. doi:10.1016/j.marpolbul.2008.08.005

Outram, F. N., and Hiscock, K. M. (2012). Indirect Nitrous Oxide Emissions from Surface Water Bodies in a Lowland Arable Catchment: A Significant Contribution to Agricultural Greenhouse Gas Budgets. *Environ. Sci. Technol.* 46 (15), 8156–8163. doi:10.1021/es3012244

Qu, B., Aho, K. S., Li, C., Kang, S., Sillanpää, M., Yan, F., et al. (2017). Greenhouse gases emissions in rivers of the Tibetan Plateau. *Sci. Rep.* 7 (1), 16573. doi:10.1038/s41598-017-16552-6

Ravishankara, A. R., Daniel, J. S., and Portmann, R. W. (2009). Nitrous oxide (N2O): the dominant ozone-depleting substance emitted in the 21st century. *Science* 326 (5949), 123–125. doi:10.1126/science.1176985

Raymond, P. A., and Cole, J. J. (2001). Gas Exchange in Rivers and Estuaries: Choosing a Gas Transfer Velocity. *Estuaries* 24, 312–317. doi:10.2307/1352954

Ren, H., Yuan, X., Yue, J., Wang, X., and Liu, H. (2016). Potholes of Mountain River as Biodiversity Spots: Structure and Dynamics of the Benthic Invertebrate Community. *Polish J. Ecol.* 64 (1), 70–83. doi:10.3161/15052249pje2016.64.1.007

Rosamond, M. S., Thuss, S. J., and Schiff, S. L. (2012). Dependence of riverine nitrous oxide emissions on dissolved oxygen levels. *Nat. Geosci.* 5 (10), 715–718. doi:10.1038/ngeo1556

Rosamond, M. S., Thuss, S. J., Schiff, S. L., and Elgood, R. J. (2011). Coupled cycles of dissolved oxygen and nitrous oxide in rivers along a trophic gradient in southern Ontario, Canada. *J. Environ. Qual.* 40 (1), 256–270. doi:10.2134/jeq2010.0009

Saunders, D. L., and Kalff, J. (2001). Nitrogen retention in wetlands, lakes and rivers. *Hydrobiologia* 443 (1-3), 205–212. doi:10.1023/A:1017506914063

Seitzinger, S. P., Kroeze, C., and Styles, R. V. (2000). Global distribution of N2O emissions from aquatic systems: natural emissions and anthropogenic effects. *Chemosphere - Glob. Change Sci.* 2, 267–279. doi:10.1016/S1465-9972(00)00015-5

Shi, W., Chen, Q., Yi, Q., Yu, J., Ji, Y., Hu, L., et al. (2017). Carbon Emission from Cascade Reservoirs: Spatial Heterogeneity and Mechanisms. *Environ. Sci. Technol.* 51 (21), 12175–12181. doi:10.1021/acs.est.7b03590

Shi, W., Chen, Q., Zhang, J., Liu, D., Yi, Q., Chen, Y., et al. (2020). Nitrous oxide emissions from cascade hydropower reservoirs in the upper Mekong River. *Water Res.* 173, 115582. doi:10.1016/j.watres.2020.115582

Silvennoinen, H., Liikanen, A., Rintala, J., and Martikainen, P. J. (2008a). Greenhouse gas fluxes from the eutrophic Temmesjoki River and its Estuary in the Liminganlahti Bay (the Baltic Sea). *Biogeochemistry* 90 (2), 193–208. doi:10.1007/s10533-008-9244-1

Silvennoinen, H., Liikanen, A., Torssonen, J., Stange, C. F., and Martikainen, P. J. (2008b). Denitrification and N2O effluxes in the Bothnian Bay (northern Baltic Sea) river sediments as affected by temperature under different oxygen concentrations. *Biogeochemistry* 88 (1), 63–72. doi:10.1007/s10533-008-9194-7

Smensen, J., Jmgensen, T., and Brandt, S. (1988). Denitrification in stream epilithon Seasonal variation in Gelbk and Rabis Bk, Denmark. *FEMS Microbiol. Lett.* 53 (6), 345–353. doi:10.1016/0378-1097(88)90500-910.1111/j.1574-6968.1988.tb02749.x

Soued, C., del Giorgio, P. A., and Maranger, R. (2015). Nitrous oxide sinks and emissions in boreal aquatic networks in Québec. *Nat. Geosci.* 9 (2), 116–120. doi:10.1038/ngeo2611

Stow, C. A., Walker, J. T., Cardoch, L., Spence, P., and Geron, C. (2005). N2O Emissions from Streams in the Neuse River Watershed, North Carolina. *Environ. Sci. Technol.* 39 (18), 6999–7004. doi:10.1021/es0500355

Tingting, L., Wang, X. f., Xiaofeng, W., Xingzhong, Y., Xiaojie, G., Chunli, H., et al. (2019). Review on N2O emission from lakes and reservoirs. *J. Lake Sci.* 31 (2), 319–335. doi:10.18307/2019.0202

Trauth, N., Musolff, A., Knöller, K., Kaden, U. S., Keller, T., Werban, U., et al. (2018). River water infiltration enhances denitrification efficiency in riparian groundwater. *Water Res.* 130, 185–199. doi:10.1016/j.watres.2017.11.058

Van Cappellen, P., and Maavara, T. (2016). Rivers in the Anthropocene: Global scale modifications of riverine nutrient fluxes by damming. *Ecohydrology & Hydrobiology* 16 (2), 106–111. doi:10.1016/j.ecohyd.2016.04.001

Wang, D., Chen, Z., Sun, W., Hu, B., and Xu, S. (2009a). Methane and nitrous oxide concentration and emission flux of Yangtze Delta plain river net. *Sci. China Ser. B-chem.* 52 (5), 652–661. doi:10.1007/s11426-009-0024-0

Wang, F. (2020). Impact of a large sub-tropical reservoir on the cycling of nutrients in a river. *Water Res.* 186, 116363. doi:10.1016/j.watres.2020.116363

Wang, F., Maberly, S. C., Wang, B., and Liang, X. (2018a). Effects of dams on riverine biogeochemical cycling and ecology. *Inland Waters* 8 (2), 130–140. doi:10.1080/20442041.2018.1469335

Wang Qiang, 王., Pang Xu, 庞., Li Xiuming, 李., Wang Zhijian, 王., Yuan Xingzhong, 袁., and Zhang Yaoguang, 张. (2019). Assessment method for the influence of hydroelectric dams on the physical habitat quality and longitudinal connectivity of rivers: a case study of the Wubu and Zaodu rivers. *Acta Eco Sin* 39 (15), 5508–5516. doi:10.5846/stxb201808261822

Wang, S., Liu, C., Yeager, K. M., Wan, G., Li, J., Tao, F., et al. (2009b). The spatial distribution and emission of nitrous oxide (N2O) in a large eutrophic lake in eastern China: Anthropogenic effects. *Sci. Total Environ.* 407 (10), 3330–3337. doi:10.1016/j.scitotenv.2008.10.037

Wang, X., He, Y., Yuan, X., Chen, H., Peng, C., Yue, J., et al. (2017a). Greenhouse gases concentrations and fluxes from subtropical small reservoirs in relation with watershed urbanization. *Atmos. Environ.* 154, 225–235. doi:10.1016/j.atmosenv.2017.01.047

Wang, Z.-J., Yue, F.-J., Li, S.-L., Li, X.-D., Wang, S.-L., Li, C., et al. (2018b). Nitrate dynamics during impoundment and flood periods in a subtropical karst reservoir: Hongfeng Lake, Southwestern China. *Environ. Sci. Process. Impacts* 20 (12), 1736–1745. doi:10.1039/c8em00445e

Wanninkhof, R. (1992). Relationship between wind speed and gas exchange over the ocean. *J. Geophys. Res.* 97 (C5), 7373. doi:10.1029/92jc00188

Weiss, R. F., and Price, B. A. (1980). Nitrous Oxide Solubility in Water and Seawater. *Mar. Chem.* 8 (4), 347–359. doi:10.1016/0304-4203(80)90024-9

Wenk, C. B., Frame, C. H., Koba, K., Casciotti, K. L., Veronesi, M., Niemann, H., et al. (2016). Differential N2 O dynamics in two oxygen-deficient lake basins

revealed by stable isotope and isotopomer distributions. *Limnol. Oceanogr.* 61 (5), 1735–1749. doi:10.1002/lno.10329

World Meteorological Organization (2019). *WMO Greenhouse Gas Bulletin: The State of Greenhouse Gases in the Atmosphere Based on Global Observations through 2018*.

Wu, W., Wang, J., Zhou, X., Yuan, B., Guo, M., and Ren, L. (2020). Spatiotemporal distribution of nitrous oxide (N 2 O) emissions from cascade reservoirs in Lancang-Mekong River Yunnan section, Southwestern China. *River Res. Applic*, 1–15. doi:10.1002/rra.3726

Yan, W., Mayorga, E., Li, X., Seitzinger, S. P., and Bouwman, A. F. (2010). Increasing anthropogenic nitrogen inputs and riverine DIN exports from the Changjiang River basin under changing human pressures. *Glob. Biogeochem. Cycles* 24 (4), a–n. doi:10.1029/2009gb003575

Yan, W., Yang, L., Wang, F., Wang, J., and Ma, P. (2012). Riverine N 2 O concentrations, exports to estuary and emissions to atmosphere from the Changjiang River in response to increasing nitrogen loads. *Glob. Biogeochem. Cycles* 26 (4), 1–14. doi:10.1029/2010gb003984

Yang, D., Mao, X., Wei, X., Tao, Y., Zhang, Z., and Ma, J. (2020). Water-Air Interface Greenhouse Gas Emissions (CO2, CH4, and N2O) Emissions Were Amplified by Continuous Dams in an Urban River in Qinghai-Tibet Plateau, China. *Water* 12 (3), 759. doi:10.3390/w12030759

Yang, M., Geng, X. M., Grace, J., Jia, Y. F., Liu, Y. Z., Jiao, S. W., et al. (2015). Responses of N2O flux to water level fluctuation and other environmental factors at littoral zone of Miyun Reservoir: a comparison with CH4 fluxes. *Biogeosciences Discuss.* 12 (7), 5333–5363. doi:10.5194/bgd-12-5333-2015

Yang Ping, 杨., and Tong Chuan, 仝. (2015). Emission paths and measuring methods of greenhouse gases fluxes from fresh-water aquatic ecosystems: A review. *Acta Eco Sin* 35 (20), 6868–6880. doi:10.5846/stxb201406231298

Ye, W., Bian, L., Wang, C., Zhu, R., Zheng, X., and Ding, M. (2016). Monitoring atmospheric nitrous oxide background concentrations at Zhongshan Station, east Antarctica. *J. Environ. Sci.* 47, 193–200. doi:10.1016/j.jes.2015.12.038

Yu, Z., Deng, H., Wang, D., Ye, M., Tan, Y., Li, Y., et al. (2013). Nitrous oxide emissions in the Shanghai river network: implications for the effects of urban sewage and IPCC methodology. *Glob. Change Biol.* 19 (10), 2999–3010. doi:10.1111/gcb.12290

Zhou, X., Chen, N., Yan, Z., and Duan, S. (2016). Warming increases nutrient mobilization and gaseous nitrogen removal from sediments across cascade reservoirs. *Environ. Pollut.* 219, 490–500. doi:10.1016/j.envpol.2016.05.060

Zhu, D., Chen, H., Yuan, X., Wu, N., Gao, Y., Wu, Y., et al. (2013). Nitrous oxide emissions from the surface of the Three Gorges Reservoir. *Ecol. Eng.* 60, 150–154. doi:10.1016/j.ecoleng.2013.07.049

Zhu, D., Wu, Y., Wu, N., Chen, H., He, Y., Zhang, Y., et al. (2015). Nitrous oxide emission from infralittoral zone and pelagic zone in a shallow lake: Implications for whole lake flux estimation and lake restoration. *Ecol. Eng.* 82, 368–375. doi:10.1016/j.ecoleng.2015.05.032

Conflict of Interest: The authors declare that the research was conducted in the absence of any commercial or financial relationships that could be construed as a potential conflict of interest.

Publisher's Note: All claims expressed in this article are solely those of the authors and do not necessarily represent those of their affiliated organizations or those of the publisher, the editors, and the reviewers. Any product that may be evaluated in this article or claim that may be made by its manufacturer is not guaranteed or endorsed by the publisher.